Thrombosis Research (2008) 122, 179–184

ELSEVIER

THROMBOSIS RESEARCH

intl.elsevierhealth.com/journals/thre

BRIEF COMMUNICATION

No association between vitamin K epoxide reductase complex subunit 1-like 1 (*VKORC1L1*) and the variability of warfarin dose requirement in a Japanese patient population

Tong Yin [a], Hironori Hanada [a], Kotaro Miyashita [b], Yoshihiro Kokubo [c], Yasuhisa Akaiwa [b], Ryoichi Otsubo [b], Kazuyuki Nagatsuka [b], Toshiho Otsuki [b], Akira Okayama [c], Kazuo Minematsu [b], Hiroaki Naritomi [b], Hitonobu Tomoike [c], Toshiyuki Miyata [a,*]

[a] *Research Institute, National Cardiovascular Center, 5-7-1 Fujishirodai, Suita, Osaka 565-8565, Japan*
[b] *Cerebrovascular Division, Department of Medicine, National Cardiovascular Center, Osaka, Japan*
[c] *Department of Preventive Cardiology, National Cardiovascular Center, Osaka, Japan*

Received 29 June 2007; received in revised form 15 September 2007; accepted 15 September 2007
Available online 21 February 2008

Introduction

Warfarin therapy management is challenging due to the greater than 10-fold interindividual variability in the therapeutic dose [1–4]. Haplotypes in the gene of vitamin K epoxide reductase complex (*VKORC1*), encoding vitamin K epoxide reductase which is a target enzyme of warfarin, have been linked to the effective maintenance dose of warfarin [5–8]. Vitamin K epoxide reductase complex subunit 1-like 1 (*VKORC1L1*) is a paralogous gene of *VKORC1* and shares about 50% amino acid identity with VKORC1 protein [9,10]. The active sites of VKORC1 are predicted to reside at the thioredoxin-like Cys132-X-X-Cys135 center embedded in the transmembrane region, and the mutagenesis at one of Cys residues lost their activity [11,12]. A recent study suggested that the complex's protein disulfide isomerase subunit provides electrons for the reduction of the Cys132-X-X-Cys135 center in VKORC1 [13]. The Cys132-X-X-Cys135 center in VKORC1 is perfectly conserved in *VKORC1L1* [9,10], suggesting the functional importance of the VKORC1L1 protein as a reductase for vitamin K recycling. However, the function of VKORC1L1 is totally unknown, including whether or not the *VKORC1L1* genotypes are associated with the variability of the effective warfarin dose [14].

The International HapMap Project has deposited the patterns of more than 1 million single nucleotide polymorphisms (SNPs) in the genome sequences drawn from four diverse human populations including Japanese, with the data now available worldwide [15]. This data offer new tools for identifying phenotype-related genes and disease-causing genes in humans.

* Corresponding author. Tel.: +81 6 6833 5012x2512; fax: +81 6 6835 1176.
E-mail address: miyata@ri.ncvc.go.jp (T. Miyata).

0049-3848/$ - see front matter
doi:10.1016/j.thromres.2007.09.015

Table 1 Characteristics of patients administered warfarin maintenance dose

Number	87
Male/Female	62/25
Age (years)	67.60±10.60
Weight (kg)	60.20±9.40
Warfarin dose (mg/day)	3.00±1.03
Warfarin dose range (mg/day)	1.25–5.50

Age, weight, and warfarin dose are shown as mean±SD.

In the present study, we constructed haplotype blocks for the *VKORC1L1* gene in a Japanese population using HapMap data and investigated the influence of 8 SNPs in the haplotype blocks on the interindividual variability of warfarin dose. Our data showed that none of the SNPs and haplotypes in the *VKORC1L1* gene showed an association with the variability of the daily warfarin maintenance dose.

Materials and methods

Haplotype block construction and selection of tag SNPs

The *VKORC1L1* gene is located on chromosome 7q11.21 and ranges from 64,975,692 to 65,057,237 bp on the NCBI Build 36 assembly. HapMap data regarding the NCBI Build 36 assembly covering 200 kb length centered on the *VKORC1L1* gene for 45 normal Japanese singletons were downloaded. Haplotype blocks were constructed using Haploview version 3.32 software (http://www.broad.mit.edu/mpg/haploview/index.php) [16]. Strong linkage disequilibrium between a pair of SNPs was defined by r^2 ranging from 0.7 to 0.98. A block was created if 95% of the informative comparisons were in strong linkage disequilibrium. The block-by-block tag SNPs were selected based on Paul de Bakker's Tagger [17] with an LOD score cutoff of 3.0 and r^2 a threshold of 0.80. Frequencies of the constructed haplotype blocks and selected tag SNPs were re-confirmed using SNPAlyze v4.0 software (DYNACOM, Kanagawa, Japan).

Genotyping of selected tag SNPs in patients with warfarin dose

The study population consisted of 87 unrelated Japanese patients admitted to the Cerebrovascular Division of the National Cardiovascular Center between November 2003 and March 2004. The patients had all experienced an ischemic stroke within the 7 days prior to admission. Anticoagulation of all patients was stably controlled with a target international normalized ratio of 1.6–2.6 for the prevention of stroke recurrence [18,19]. Inclusion criteria were a confirmed date of initial exposure to warfarin and current anticoagulation therapy. Data collection consisted of inpatient and outpatient medical records. The anticoagulant database was used to obtain information on daily warfarin doses. The patient group had been previously studied for the association of four genes—*VKORC1*, γ-glutamyl carboxylase, calumenin, and *CYP2C9*—with the warfarin maintenance dose [20]. In the present study, we

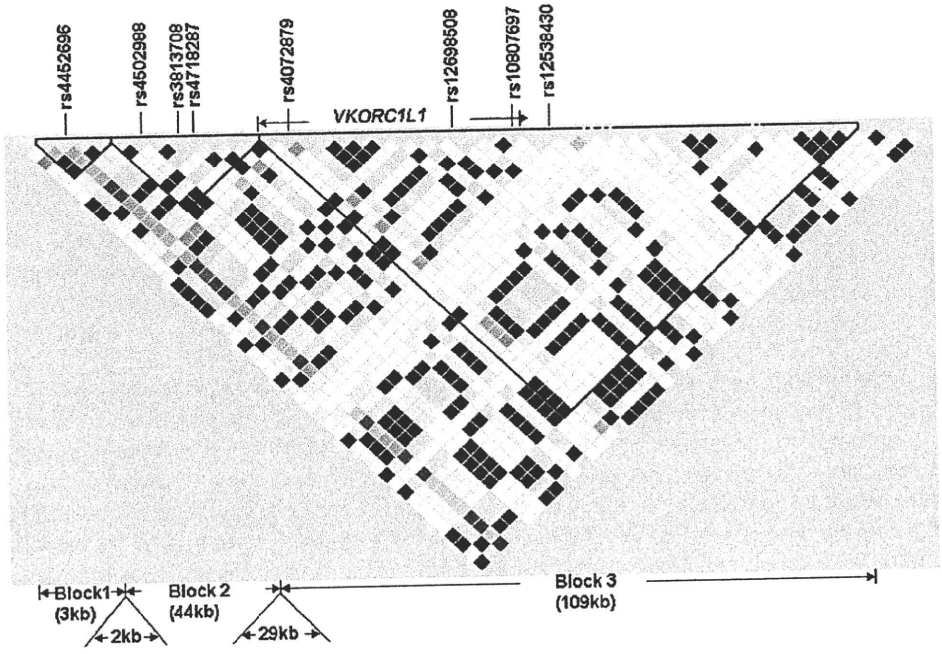

Figure 1 Haploview analysis of linkage disequilibrium structure and haplotype blocks centered on *VKORC1L1*. Pairwise linkage disequilibrium in r^2 was derived from 45 Japanese individuals (HapMap Data phase II, on NCBI Build 36 assembly). Shading represents the magnitude and significance of linkage disequilibrium, with the black-to-white gradient reflecting higher to lower linkage disequilibrium values. Three haplotype blocks were constructed covering a 200 kb length centered on the *VKORC1L1* gene. Based on the strength of linkage disequilibrium among SNP pairs, one SNP tagging the 3-kb block 1, three SNPs tagging the 44-kb block 2, and 4 SNPs tagging the 109-kb block 3 were identified. The interval length is 2 kb between blocks 1 and 2, and 29 kb between blocks 2 and 3. *VKORC1L1* is partly encompassed by block 3.

Table 2 Differences in daily warfarin dose for each SNP of the *VKORC1L1* gene

rs number	Position in reference sequence (bp)	SNP location	Genotype	Allele frequency	*n*	Mean±SD (mg/day)	*p*
rs4452696	64924147	upstream	AA	A/G	39	3.00±1.05	0.17
			AG	0.71/0.29	41	3.12±1.05	
			GG		7	2.32±0.61	
rs4502988	64935181	upstream	GG	G/A	63	2.99±1.03	0.87
			GA	0.89/0.11	24	3.03±1.07	
			AA		0	–	
rs3813708[a]	64943067	upstream	GG	G/T	60	3.07±1.05	0.44
			GT	0.83/0.17	26	2.89±0.99	
			TT		0	–	
rs4718287[b]	64944462	upstream	CC	C/G	20	3.05±1.18	0.70
			CG	0.49/0.51	40	2.90±0.95	
			GG		27	3.11±1.07	
rs4072879	65011286	intron 1	TT	T/C	47	2.96±0.90	0.93
			TC	0.76/0.24	36	3.01±1.18	
			CC		3	3.17±1.53	
rs12698508[a]	65049393	intron 1	AA	A/T	60	3.07±1.05	0.46
			AT	0.83/0.17	25	2.89±1.01	
			TT		1	1.75	
rs10807697	65053605	intron 2	AA	A/G	2	2.63±0.53	0.82
			AG	0.13/0.87	24	3.07±1.60	
			GG		61	2.99±1.05	
rs12538430[b]	65057623	3′ UTR	CC	C/T	18	3.09±1.24	0.55
			CT	0.49/0.51	40	2.87±0.93	
			TT		29	3.13±1.05	

Positions of SNPs in reference sequence are derived from NCBI Mapview Build 36. 2.
P values were calculated by one-way analysis of variance.
UTR: untranslated region. Warfarin daily maintenance dose are shown as mean±SD.
[a] SNPs were in linkage disequilibrium with $r^2=1$.
[b] These SNPs were in linkage disequilibrium with $r^2=0.99$.

genotyped 8 SNPs in *VKORC1L1*—rs4452696, rs4502988, rs3813708, rs4718287, rs4072879, rs12698508, rs10807697, and rs12538430—in the same patient group using the TaqMan-PCR system as previously described [21]. The PCR primers and probes used for the TaqMan system are available on request. We also resequenced directly the exon 1 and promoter regions of *VKORC1L1*, which were not covered by the constructed haplotype blocks, in all the patients. This study was approved by the Ethical Review Committee of the National Cardiovascular Center. All patients who participated in the study provided written informed consent for genetic analysis.

Statistical methods

All SNPs identified were tested for deviations from the Hardy–Weinberg disequilibrium through the use of a chi-square test. Pair-wise linkage disequilibrium between two SNPs was evaluated by r^2. Individual diplotype was estimated by means of an expectation maximization algorithm using SNPAlyze v4.0 software. The association of the genotypes and the inferred haplotypes with daily warfarin doses was examined by one-way analysis of variance. Statistical analyses were performed using Prism4 (GraphPad, San Diego, CA) and JMP V 5.1 software and the SAS release 8.2 (SAS Institute Inc., Cary, NC). *P* values lower than 0.05 were considered to be statistically significant. The association of the genotypes with daily warfarin doses was reconfirmed by quantitative associ-

Table 3 Differences in daily warfarin dose for each haplotype of the *VKORC1L1* gene

Haplotype sequence[a]	Genotype	*n*	Mean±SD (mg/day)	*p*
AGGCTAGC	homo	6	3.04±0.49	0.49
	hetero	20	2.74±1.10	
	none	58	3.06±1.06	
AGGCCAGC	homo	3	3.17±1.53	0.95
	hetero	34	2.96±1.19	
	none	47	2.98±0.91	
AGGGTAGT	homo	4	3.06±1.16	0.14
	hetero	32	3.26±1.00	
	none	48	2.79±1.03	
GGTGTTGT	homo	1	1.75	
	hetero	22	2.77±1.06	0.30
	none	61	3.04±1.03	
GAGGTAAT	homo	0	–	
	hetero	24	3.03±1.07	0.79
	none	60	2.96±1.04	

[a]For each haplotype sequence, SNPs are listed in sequential order as rs4452696, rs4502988, rs3813708, rs4718287, rs4072879, rs12698508, rs10807697, and rs12538430.
P values were calculated by one-way analysis of variance.
Warfarin daily maintenance dose are shown as Mean±SD.

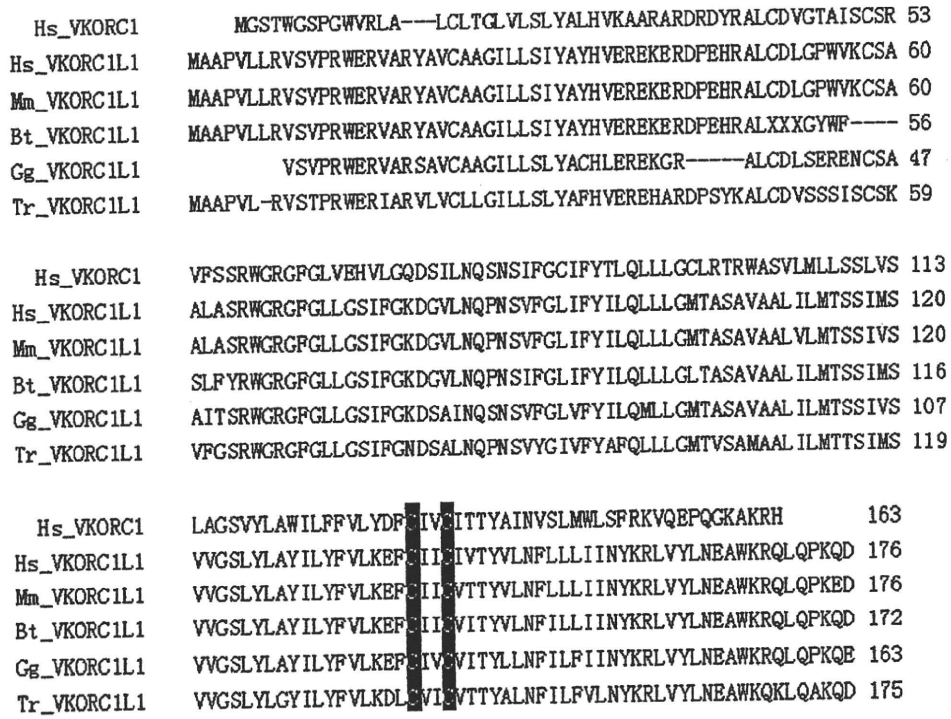

Figure 2 Amino acid sequence alignment of VKORC1L1 proteins from different species and from human VKORC1 protein. The proteins are labeled by their gene symbols and a prefix indicating the species (Hs, *Homo sapiens*; Mm, *Mus musculus*; Bt, *Bos taurus*; Gg, *Gallus gallus*; Tr, *Takifugu rubripes*). MultAlin (http://bioinfo.genopole-toulouse.prd.fr/multalin/) was used to perform the sequence alignment. Hyphens represent the amino acid deletion in the sequences. The active site Cys residues in the Cys132-X-X-Cys135 center of VKORC1 protein are indicated by a black background. The Cys-X-X-Cys center is highly conserved in VKORC1L1 proteins from various species.

ation test using the PLINK v 0.99p software (http://pngu.mgh.harvard.edu/purcell/plink/).

Results

Patient characteristics are summarized in Table 1. A total of 78 SNPs in the region of 200 kb centered on *VKORC1L1* in 45 normal Japanese has been retrieved from the Phase II HapMap data. Three haplotype blocks were constructed using 41 SNPs on Haploview, as shown in Fig. 1. The interval length between block 1 and 2 was 2 kb and between block 2 and 3 was 29 kb. Block 2 covered the putative promoter region of *VKORC1L1* (except for the 1.4 kb length of sequence in the upstream of exon 1), and block 3 included the region from intron 1 to exon 3 of *VKORC1L1*. Thus, three haplotype blocks covered the gene of *VKORC1L1* except for exon 1.

We identified 8 tag SNPs in three haplotype blocks, as shown in Fig. 1. One SNP, rs4452696, resided in block 1, three SNPs—rs4502988, rs3813708, and rs4718287—in block 2, and four SNPs—rs4072879, rs12698508, rs10807697, and rs12538430—were presented in block 3. Haplotype frequencies and selected tag SNPs were confirmed independently by means of Haplotype Inference analysis.

We genotyped 8 tag SNPs of *VKORC1L1* in 87 patients with warfarin dose. None of the SNPs showed genotype deviations from the Hardy–Weinberg equilibrium ($p>0.1$). Two pairs of SNPs (rs3813708 vs rs12698508, and rs4718287 vs rs12538430) were in tight linkage disequilibrium with r^2 values of more than 0.99, which were consistent with HapMap Phase II dataset. Comparisons of minor allele frequency between those found in the current study and those found in the HapMap dataset showed no significant differences ($p>0.2$).

None of the SNPs exhibited a significant association with the effective daily maintenance dose of warfarin (Table 2). These results were reconfirmed by the PLINK quantitative association test ($p>0.36$). Five haplotypes were estimated to show a frequency of more than 0.05. None of these haplotypes demonstrated a significant association with the variability of the daily warfarin maintenance dose (Table 3).

The exon 1 and part of the promoter regions of *VKORC1L1* were not covered by the constructed haplotype blocks, we sequenced these regions in all the patients, and a total of 9 SNPs were detected with minor allele frequency ranged from 0.05 to 0.15. No SNP could be detected in the coding region of exon 1. Association analysis showed that none of the detected SNPs had a significant association with the effective daily maintenance dose of warfarin ($p>0.22$, data not shown).

Discussion

The genes of *VKORC1* (encoding a warfarin target enzyme) and *CYP2C9* (encoding a warfarin metabolizing enzyme) are well established genetic factors for affecting inter-individual variability of the maintenance dose of warfarin [3]. VKORC1 protein

shows a reductase activity for conversion of vitamin K epoxide to vitamin K and vitamin K to vitamin KH2, which is essential for γ-glutamyl carboxylation of vitamin K dependent clotting factors [22]. *VKORC1L1* is a paralogous gene of *VKORC1*. Human VKORC1 and VKORC1L1 showed about 50% identity at the amino acid level, and the Cys-X-X-Cys center in VKORC1 is perfectly conserved in VKORC1L1. The amino acid sequence of VKORC1L1 among five different species showed 58% identity (102/176 residues) (Fig. 2).

In our previous study, we sequenced the entire coding regions of the *VKORC1* gene in order to identify the genetic variations and genotyped SNPs in relation to the daily warfarin maintenance dose in a Japanese population. We found that the *VKORC1* genotype can explain an approximately 0.9 mg daily interindividual difference in warfarin maintenance dose [20–23]. In the present study, we utilized the same patient group to evaluate the contribution of the tagging SNPs and the haplotypes of *VKORC1L1* for the interindividual variability of warfarin dose. However, no association of the *VKORC1L1* genotype with warfarin dose requirement was found. Two well known functional SNPs, *CYP2C9*3* and *VKORC1* 1173 C>T, might mask the effect of *VKORC1L1* genotype on the warfarin effective dose. To eliminate this possibility, we analyzed the association of the tagging SNPs and the haplotypes of *VKORC1L1* with interindividual variability of the daily warfarin maintenance dose in 67 patients who did not carry the variations of *CYP2C9*3* and *VKORC1* 1173 C>T. Unfortunately, significant association still could not be found ($p>0.13$, data not shown). These results suggested that *VKORC1L1* is not likely to be involved in the interindividual variability of the therapeutic dose of warfarin.

Tagging SNPs selected on the basis of HapMap data could be most effective only for the common potential functional sequence variations (more than 5% frequency) in the gene [24]. Resequencing the whole *VKORC1L1* gene would be imperative, and alternative ways for finding associations of rare variations (less than 5% frequency) with strong deleterious functional effects to the phenotype of warfarin dose would be necessary [25].

Summary

The *VKORC1* gene has been claimed to determine the interindividual variability in the maintenance dose of warfarin, but it is unknown whether the *VKORC1L1* gene, a paralogous gene of *VKORC1*, sharing about 50% amino acid identity with VKORC1 protein, also plays a role in the variability of warfarin dose. Our goal was to study the association of the *VKORC1L1* haplotypes with the warfarin maintenance dose. After constructing haplotype blocks covering a 200 kb length centered on the *VKORC1L1* gene using HapMap data in a Japanese population, we selected eight common tag SNPs in three haplotype blocks and genotyped them in 87 patients on stable anticoagulation with a target international normalized ratio of 1.6–2.6. None of the SNPs or haplotypes exhibited a significant association with the effective daily warfarin dose. Although the VKORC1L1 protein exhibits a significant amino acid identity with the VKORC1 protein, no association could be found between the *VKORC1L1* genotype and the variability of the warfarin dose in a Japanese patient population. The genotypes of this gene denied a role in the interindividual variability of the effects of warfarin. Further functional analysis of *VKORC1L1* is warranted.

Conflict of interest

We do not have any direct and indirect conflicts of interest.

Acknowledgements

This study was supported by the Program for Promotion of Fundamental Studies in Health Sciences of the National Institute of Biomedical Innovation (NIBIO) of Japan and by Grants-in-Aid from the Ministry of Health, Labor, and Welfare of Japan, and the Ministry of Education, Culture, Sports, Science, and Technology of Japan.

Tong Yin, M.D., is a recipient of Takeda Foundation, from Institute of Geriatric Cardiology, General Hospital of People's Liberation Army, Beijing, China.

References

[1] Hirsh J, Fuster V, Ansell J, Halperin JL. American Heart Association/American College of Cardiology Foundation guide to warfarin therapy. *Circulation* 2003;**107**:1692–711.

[2] Gage BF. Pharmacogenetics-based coumarin therapy. *Hematology Am Soc Hematol Educ Program* 2006:467–73.

[3] Yin T, Miyata T. Warfarin dose and the pharmacogenomics of CYP2C9 and VKORC1–rationale and perspectives. *Thromb Res* 2007;**120**:1–10.

[4] Millican E, Jacobsen-Lenzini PA, Milligan PE, Grosso L, Eby C, Deych E, Grice G, Clohisy JC, Barrack RL, Burnett RS, Voora D, Gatchel S, Tiemeier A, Gage BF. Genetic-based dosing in orthopaedic patients beginning warfarin therapy. *Blood* 2007;**110**:1511–5.

[5] Rieder MJ, Reiner AP, Gage BF, Nickerson DA, Eby CS, McLeod HL, Blough DK, Thummel KE, Veenstra DL, Rettie AE. Effect of VKORC1 haplotypes on transcriptional regulation and warfarin dose. *N Engl J Med* 2005;**352**:2285–93.

[6] Geisen C, Watzka M, Sittinger K, Steffens M, Daugela L, Seifried E, Muller CR, Wienker TF, Oldenburg J. VKORC1

haplotypes and their impact on the inter-individual and inter-ethnical variability of oral anticoagulation. *Thromb Haemost* 2005;**94**:773–9.

[7] Marsh S, King CR, Porche-Sorbet RM, Scott-Horton TJ, Eby CS. Population variation in VKORC1 haplotype structure. *J Thromb Haemost* 2006;**4**:473–4.

[8] Osman A, Enstrom C, Arbring K, Soderkvist P, Lindahl TL. Main haplotypes and mutational analysis of vitamin K epoxide reductase (VKORC1) in a Swedish population: a retrospective analysis of case records. *J Thromb Haemost* 2006;**4**:1723–9.

[9] Rost S, Fregin A, Ivaskevicius V, Conzelmann E, Hortnagel K, Pelz HJ, Lappegard K, Seifried E, Scharrer I, Tuddenham EG, Muller CR, Strom TM, Oldenburg J. Mutations in VKORC1 cause warfarin resistance and multiple coagulation factor deficiency type 2. *Nature* 2004;**427**:537–41.

[10] Li T, Chang CY, Jin DY, Lin PJ, Khvorova A, Stafford DW. Identification of the gene for vitamin K epoxide reductase. *Nature* 2004;**427**:541–4.

[11] Wajih N, Sane DC, Hutson SM, Wallin R. Engineering of a recombinant vitamin K-dependent gamma-carboxylation system with enhanced gamma-carboxyglutamic acid forming capacity: evidence for a functional CXXC redox center in the system. *J Biol Chem* 2005;**280**:10540–7.

[12] Rost S, Fregin A, Hunerberg M, Bevans CG, Muller CR, Oldenburg J. Site-directed mutagenesis of coumarin-type anticoagulant-sensitive VKORC1: evidence that highly conserved amino acids define structural requirements for enzymatic activity and inhibition by warfarin. *Thromb Haemost* 2005;**94**:780–6.

[13] Wajih N, Hutson SM, Wallin R. Disulfide-dependent protein folding is linked to operation of the vitamin K cycle in the endoplasmic reticulum. A protein disulfide isomerase-VKORC1 redox enzyme complex appears to be responsible for vitamin K1 2,3-epoxide reduction. *J Biol Chem* 2007;**282**:2626–35.

[14] Wadelius M, Chen LY, Eriksson N, Bumpstead S, Ghori J, Wadelius C, Bentley D, McGinnis R, Deloukas P. Association of warfarin dose with genes involved in its action and metabolism. *Hum Genet* 2007;**121**:23–34.

[15] Consortium. TIH. A haplotype map of the human genome. *Nature* 2005;**437**:1299–320.

[16] Barrett JC, Fry B, Maller J, Daly MJ. Haploview: analysis and visualization of LD and haplotype maps. *Bioinformatics* 2005;**21**:263–5.

[17] de Bakker PI, Yelensky R, Pe'er I, Gabriel SB, Daly MJ, Altshuler D. Efficiency and power in genetic association studies. *Nat Genet* 2005;**37**:1217–23.

[18] Yamaguchi T. Optimal intensity of warfarin therapy for secondary prevention of stroke in patients with nonvalvular atrial fibrillation: a multicenter, prospective, randomized trial. Japanese Nonvalvular Atrial Fibrillation-Embolism Secondary Prevention Cooperative Study Group. *Stroke* 2000;**31**:817–21.

[19] Chimowitz MI, Lynn MJ, Howlett-Smith H, Stern BJ, Hertzberg VS, Frankel MR, Levine SR, Chaturvedi S, Kasner SE, Benesch CG, Sila CA, Jovin TG, Romano JG. Comparison of warfarin and aspirin for symptomatic intracranial arterial stenosis. *N Engl J Med* 2005;**352**:1305–16.

[20] Kimura R, Miyashita K, Kokubo Y, Akaiwa Y, Otsubo R, Nagatsuka K, Otsuki T, Okayama A, Minematsu K, Naritomi H, Honda S, Tomoike H, Miyata T. Genotypes of vitamin K epoxide reductase, gamma-glutamyl carboxylase, and cytochrome P450 2C9 as determinants of daily warfarin dose in Japanese patients. *Thromb Res* 2007;**120**:181–6.

[21] Tanaka C, Kamide K, Takiuchi S, Miwa Y, Yoshii M, Kawano Y, Miyata T. An alternative fast and convenient genotyping method for the screening of angiotensin converting enzyme gene polymorphisms. *Hypertens Res* 2003;**26**:301–6.

[22] Chu PH, Huang TY, Williams J, Stafford DW. Purified vitamin K epoxide reductase alone is sufficient for conversion of vitamin K epoxide to vitamin K and vitamin K to vitamin KH2. *Proc Natl Acad Sci U S A* 2006;**103**:19308–13.

[23] Kimura R, Kokubo Y, Miyashita K, Otsubo R, Nagatsuka K, Otsuki T, Sakata T, Nagura J, Okayama A, Minematsu K, Naritomi H, Honda S, Sato K, Tomoike H, Miyata T. Polymorphisms in vitamin K-dependent gamma-carboxylation-related genes influence interindividual variability in plasma protein C and protein S activities in the general population. *Int J Hematol* 2006;**84**:387–97.

[24] Gibbs R. Deeper into the genome. *Nature* 2005;**437**:1233–4.

[25] Topol EJ, Frazer KA. The resequencing imperative. *Nat Genet* 2007;**39**:439–40.

Impact of concomitant diabetes and chronic kidney disease on preload-induced changes in left ventricular diastolic filling in hypertensive patients

Yoshio Iwashima[a], Takeshi Horio[a], Yoshihiko Suzuki[b], Takashi Takagi[c], Kei Kamide[c], Mitsuru Ohishi[c], Toshio Ogihara[d], Junichi Yoshikawa[e], Yuhei Kawano[a] and Hiromi Rakugi[c]

Objectives **Concomitant diabetes and/or chronic kidney disease (CKD) in hypertensive patients may portend additive deleterious effects on active left ventricular relaxation. We investigated the effect of a passive leg lifting (PLL) maneuver, a means of increasing preload, on left ventricular filling to assess the relationship of concomitant diabetes mellitus (DM) and/or CKD with diastolic function in hypertensive patients.**

Methods **A total of 155 asymptomatic essential hypertensive patients underwent Doppler echocardiography to compare the echocardiographic indices at baseline and during PLL. In 51 patients, the effect of physiological saline infusion was also examined.**

Results **The changes in echocardiographic indices, including deceleration time of early diastolic filling (EDT) and the ratio of transmitral early left ventricular filling velocity to early diastolic Doppler tissue imaging of the mitral annulus (E/E′) by saline infusion showed a good correlation with those induced by PLL (Bland–Altman plot and linear regression). We next divided the total participants into four groups according to the presence/absence of diabetes and/or CKD [DM(−)/CKD(−); $n = 48$, DM(+)/CKD(−); $n = 25$, DM(−)/CKD(+); $n = 43$, and DM(+)/CKD(+); $n = 39$)] and found that the changes in EDT ($F = 15.92$, $P < 0.01$) as well as those in E/E′ ($F = 8.87$, $P < 0.01$) were significantly different among the subgroups. Multiple logistic regression analysis revealed that these complications were independent predictors of EDT less than 150 ms [DM, odds ratio (OR): 2.82; CKD, OR: 2.18, $P < 0.05$, respectively] as well as E/E′ ratio at least 15.0 during PLL (DM, OR: 4.78; CKD, OR: 3.32, $P < 0.05$, respectively).**

Conclusion **This simple preloading test unmasks latent progression of left ventricular dysfunction in essential hypertension; that is, these complications potentially cause deterioration of left ventricular compliance and preload reserve even in the early stages of diastolic dysfunction.**
J Hypertens **29:144–153 © 2010 Wolters Kluwer Health | Lippincott Williams & Wilkins.**

Journal of Hypertension 2011, 29:144–153

Keywords: chronic kidney disease, complication, diabetes, diastolic function, hypertension

Abbreviations: A′-velocity, tissue Doppler late diastolic velocity; ARdur–Ad, the time difference between the duration of the atrial filling wave and the duration of flow at atrial contraction; A-velocity, the transmitral late filling velocity; CKD, chronic kidney disease; CVD, cardiovascular disease; DM, diabetes mellitus; E/A, the ratio of peak early to late diastolic filling velocity; E/E′ ratio, the ratio of early diastolic transmitral velocity to early diastolic tissue velocity; E′-velocity, tissue Doppler early diastolic velocity; EDT, the deceleration time of early diastolic left ventricular filling; eGFR, estimated glomerular filtration rate; E-velocity, the transmitral early filling velocity; HOMA index, homeostatic model assessment index; PLL, passive leg lifting; PVa, pulmonary vein atrial reversal; PVd, peak diastolic forward flow velocity; PVs, peak systolic forward flow velocity; S/D ratio, the ratio of the pulmonary venous systolic velocity to diastolic velocity; S′-velocity, tissue Doppler systolic velocity

[a]Division of Hypertension and Nephrology, Department of Medicine, National Cardiovascular Center, Osaka, [b]Department of Internal Medicine, Circulatory and Fluid Regulation, Faculty of Medicine, University of Miyazaki, Miyazaki, [c]Department of Geriatric Medicine, Osaka University Graduate School of Medicine, [d]Osaka General Medical Center, Osaka Prefectural Hospital Organization and [e]Osaka Ekisaikai Hospital, Osaka, Japan

Correspondence to Takeshi Horio, MD, PhD, Division of Hypertension and Nephrology, Department of Medicine, National Cardiovascular Center, 5-7-1 Fujishirodai, Suita, Osaka 565-8565, Japan
Tel: +81 6 6833 5012; fax: +81 6 6872 7486; e-mail: thorio@ri.ncvc.go.jp

Received 16 November 2009 Revised 1 August 2010
Accepted 9 August 2010

Introduction

It is increasingly recognized that hypertensive patients with concomitant risk factors, such as diabetes mellitus (DM) and chronic kidney disease (CKD), are at increased risk of subsequent cardiovascular disease (CVD) [1–5]. Although the mechanism of the association of concomitant DM and/or CKD in hypertension with high CVD risk remains to be elucidated, it is possible that latent left ventricular diastolic dysfunction may also be present in these patients before the development of more severe stages of diastolic dysfunction, and, thus, contribute to CVD risk.

Doppler echocardiography permits noninvasive assessment of left ventricular diastolic function in addition to measurement of systolic function. Mitral inflow velocity recorded by Doppler echocardiography has been widely used to evaluate left ventricular diastolic function [6,7]. Previous reports have shown that the baseline mitral flow pattern and its variations after loading manipulations, recorded by means of echocardiography, are a powerful prognostic marker in patients with chronic heart failure [8,9]. The passive leg lifting (PLL) maneuver is a noninvasive and cost-effective method to increase preload through a transient increase in venous return. This simple

0263-6352 © 2010 Wolters Kluwer Health | Lippincott Williams & Wilkins

DOI:10.1097/HJH.0b013e32833f387c

maneuver has several advantages over volume loading for the purpose of assessing directional changes in diastolic function, because it does not significantly affect blood pressure, heart rate, or afterload [9,10], and the duration of the effect is short [9,11]. In previous studies, this maneuver was performed only in chronic heart failure patients [8,9,11], healthy individuals [10], or open chest coronary surgery patients [12], and the prognostic value of this maneuver was explored by categorizing diastolic dysfunction according to the severity; that is, 'in heart failure patients, a restrictive filling pattern in response to PLL maneuver has a worse prognosis'. However, even in essential hypertension with left ventricular hypertrophy (LVH), a restrictive left ventricular filling pattern is very uncommon [13]. On the other hand, it is increasingly recognized that left ventricular diastolic dysfunction is more severe in patients with DM and hypertension [14], renal dysfunction such as microalbuminuria [15], and end-stage renal disease [16]. These results suggest that concomitant DM and/or renal dysfunction in hypertension portend additive deleterious effects on active left ventricular relaxation. Accordingly, the present study examined the effect of PLL maneuver on Doppler echocardiographic indices to assess the relationship of concomitant DM and/or CKD to diastolic function in hypertensive patients without previous CVD.

Methods

Study population

We studied 155 consecutive patients referred to Osaka University Hospital, Japan for evaluation of asymptomatic hypertension. Eligible patients aged 32–87 years who had good-quality echocardiographic recordings were enrolled, and all patients included in this study were in stable sinus rhythm. Hypertension was defined as SBP at least 140 mmHg and/or DBP at least 90 mmHg on repeated measurements, or receiving antihypertensive treatment. DM was defined according to the American Diabetes Association criteria [17]. CKD was defined according to the guidelines of the National Kidney Foundation classification of CKD, as estimated glomerular filtration rate (eGFR) less than 60 ml/min per 1.73 m^2 or dipstick proteinuria ($\geq$1+) [18]. Smoking status was determined by interview and defined as follows: never smoker, past smoker (history of habitual smoking but had quit), and current smoker. Ischemic heart disease was defined as a 75% or greater organic stenosis of at least one major coronary artery as confirmed by coronary angiography, or a history of myocardial infarction or percutaneous transluminal coronary angioplasty. Exclusion criteria included ischemic heart disease, acute coronary syndrome, chronic heart failure [New York Heart Association (NYHA) class II or greater], old cerebral infarction, history of transient ischemic attack, and secondary hypertension. Participants with moderate or severe aortic or mitral regurgitation, heart rate more than 100 bpm, abnormal heart rhythm, diabetic retinopathy or neuropathy, receiving hemodialysis or erythropoietin therapy, or undetectable pulmonary venous flow throughout the cardiac cycle or absent reversal were also excluded. The study protocol was approved by the Ethics Committee of Osaka University, and all procedures followed were in accordance with the institutional guidelines of Osaka University. All participants enrolled in this study were Japanese, and all gave written informed consent to participate in the study.

Baseline clinical characteristics

After fasting overnight, venous blood and urine sampling was performed in all participants. Height and body weight were measured, and BMI was calculated. The following parameters were also determined: total cholesterol, triglycerides, high-density lipoprotein cholesterol, hemoglobin A1c, and homeostatic model assessment (HOMA) index; that is, plasma glucose level $\times$ (plasma insulin level/22.5). eGFR was calculated using the abbreviated Modification of Diet in Renal Disease (MDRD) formula in ml/min per 1.73 m^2.

Echocardiographic methods and calculation of derived variables

Imaging and Doppler echocardiography were performed in all participants in this study. Studies were performed using phased-array echocardiography with M-mode, two-dimensional, pulsed, and color-flow Doppler capabilities, as previously described [19,20]. Left ventricular internal dimension and septal and posterior wall thickness were measured at end-diastole and end-systole according to the American Society of Echocardiography recommendations [21]. Color-flow Doppler recordings were used to check for aortic and mitral regurgitation, as previously described [22]. End-diastolic dimensions were used to calculate left ventricular mass by a previously reported formula [23]. Left ventricular mass was considered an unadjusted variable and was normalized by body surface area and expressed as left ventricular mass index (LVMI). LVH was considered to be present when LVMI was more than 116 g/m^2 for men and more than 104 g/m^2 for women [24,25].

The left ventricular diastolic filling pattern was recorded from the apical transducer position with the participant in the left lateral decubitus position, with the sample volume situated between the mitral leaflet tips. The leading edge of the transmitral Doppler flow pattern was traced to derive the peak of early diastolic and atrial phase left ventricular filling (E-velocity and A-velocity, respectively), E/A ratio, the deceleration time of early diastolic left ventricular filling (EDT), and the duration of the atrial filling wave (Ad).

Pulmonary venous flow velocity was recorded by placing a sample volume about 1 cm into the right superior pulmonary vein [26]. Pulmonary vein systolic (PVs),

diastolic (PVd), S/D ratio, and atrial reversal (PVa), as well as the duration of flow at atrial contraction (ARdur), were recorded. When a biphasic PVs was detected, the highest peak velocity was used [26]. Ad and ARdur were measured as close to the zero baseline as possible from the start to termination of flow at atrial contraction after the P wave on the simultaneously recorded electrocardiogram, and the difference between Ad and ARdur was calculated (ARdur−Ad).

Pulsed wave Doppler tissue imaging was also performed by activating the Doppler tissue imaging function in the same machine. Sample volume was located at the septal side of the mitral annulus. Peak mitral annular systolic (S′) and diastolic early (E′) and late (A′) tissue velocities were measured. All measurements were performed by one trained investigator who was blinded to the clinical data of the participants.

Loading manipulations

All patients underwent simultaneous measurement of blood pressure and echocardiographic parameters. Blood pressure was measured noninvasively using a calibrated semiautomatic cuff connected to a Marquette monitor. After performing Doppler echocardiographic recording as well as blood pressure measurement at baseline, loading manipulations were performed. Specifically, in all patients, measurements were repeated during a PLL maneuver (legs elevated to 45° from the horizontal position) maintained for at least 1 min. The timing of the maximum changes occurring in the transmitral and pulmonary venous flow patterns as well as left ventricular tissue velocity was determined, and blood pressure was measured simultaneously. In 51 patients, after repeat baseline measurements to confirm a return to a hemodynamic steady state (usually 10–20 min), warm (37°C) physiological saline was infused rapidly at a rate of 33 ml/min. Simultaneous blood pressure and echocardiographic measurements were repeated after 15 min (500 ml infusion).

Statistical analysis

Summary statistics are presented as mean (±SD) for continuous variables, or percentages for categorical variables unless otherwise specified. First, the significance of differences in parameters before and after loading manipulations was evaluated using paired *t*-test. To compare the difference in changes in parameters induced by the two loading manipulations between groups, two-sample *t*-test was used. Linear regression analysis was used to assess the correlation of changes in Doppler echocardiographic indices induced by the two loading manipulations. Bland–Altman analysis was used to evaluate the agreement between the two methods, and limits of agreement (mean ± 1.96 times the SD of the differences) were determined. Second, we divided the participants into four categories according to the presence/absence of DM and/or CKD. Differences in characteristics between groups were tested using χ^2 test for dichotomous variables, and one-way analysis of variance (ANOVA) with Sheffe's posttest for continuous variables, as appropriate. Third, paired *t*-test of the differences was used to compare paired measurements within groups before and after the PLL maneuver. Fourth, to determine the significance of the difference in parameters induced by PLL between subgroups, Friedman test was used. Fifth, logistic regression analysis was used to determine the odds ratio (OR) of EDT during PLL less than 150 or E/E′ ratio during PLL at least 15.0. Multivariable logistic regression analysis was used to identify independent determinants of EDT during PLL less than 150 or E/E′ ratio during PLL at least 15.0, after accounting for relevant variables using a *P* value of less than 0.05 as the selection criterion. All *P* values were two sided, and those less than 0.05 were considered statistically significant. All calculations were performed using a standard statistical package (SPSS, version 17.0; SPSS Inc., Chicago, Illinois, USA).

Results

Comparative study

Of the 155 participants, 51 consented to participate in the comparative study (31 men; mean age 67 ± 9 years, 17 without DM and CKD, 26 with DM or CKD, and eight with DM and CKD). The two loading manipulations to evaluate diastolic reserve were well tolerated without adverse events. Blood pressure, heart rate, and echocardiographic indices before and after loading manipulations with physiological saline infusion and PLL maneuver are summarized in Table 1. Blood pressure and heart rate did not change significantly. EDT was significantly decreased, and peak E-velocity, E/A ratio, peak PVs-velocity, peak PVd-velocity, peak E′-velocity, and E/E′ ratio were significantly increased in response to loading manipulations. The changes in blood pressure, heart rate, and echocardiographic indices were not significantly different between the two loading manipulations. The changes in EDT ($y = 11.08 + 0.73x$, $r = 0.85$) and E/E′ ratio ($y = -0.02 + 0.77x$, $r = 0.82$) by physiological saline infusion were strongly correlated with those induced by PLL ($P < 0.01$, respectively). Bland–Altman plot regression showed good agreement of changes in EDT (Fig. 1a) and E/E′ ratio (Fig. 1b) induced by saline infusion with those induced by PLL.

Doppler and hemodynamic characteristics at baseline and in response to passive leg lifting

Baseline clinical and biochemical characteristics of the study participants are shown in Table 2. We divided the total participants into four groups as follows: no DM and no CKD [DM(−)/CKD(−)], DM without CKD [DM(+)/CKD(−)], CKD without DM [DM(−)/CKD(+)], and DM and CKD [DM(+)/CKD(+)]. At baseline, 64 of the total participants had DM and 82 had CKD. Patients with DM(+)/CKD(+) had a worse functional status and

Table 1 Hemodynamics and echocardiographic indices at baseline and during loading manipulations in patients enrolled in comparative study

	Physiological saline		PLL		
	Baseline	Saline	Baseline	PLL	*P* value between groups
SBP (mmHg)	136.7 ± 16.3	137.2 ± 17.0	135.4 ± 13.4	137.0 ± 15.7	NS
DBP (mmHg)	76.4 ± 10.5	76.8 ± 11.0	76.0 ± 10.8	76.5 ± 11.9	NS
Heart rate (bpm)	60.1 ± 8.1	61.0 ± 8.6	61.9 ± 7.2	63.2 ± 8.1	NS
E-velocity (m/s)	0.72 ± 0.14	0.88 ± 0.14†	0.72 ± 0.14	0.87 ± 0.15†	NS
A-velocity (m/s)	0.79 ± 0.19	0.84 ± 0.20†	0.78 ± 0.18	0.80 ± 0.20	NS
E/A ratio	0.96 ± 0.26	1.08 ± 0.24†	0.96 ± 0.26	1.14 ± 0.31†	NS
EDT (ms)	235.1 ± 37.7	187.9 ± 38.1†	236.9 ± 40.5	187.4 ± 37.0†	NS
PVs-velocity (m/s)	0.55 ± 0.13	0.64 ± 0.15†	0.55 ± 0.13	0.60 ± 0.11*	NS
PVd-velocity (m/s)	0.34 ± 0.15	0.47 ± 0.15†	0.38 ± 0.13	0.41 ± 0.11†	NS
S/D ratio	1.54 ± 0.45	1.45 ± 0.42	1.58 ± 0.50	1.51 ± 0.35	NS
PVa-velocity (m/s)	0.26 ± 0.09	0.28 ± 0.04†	0.25 ± 0.06	0.27 ± 0.04	NS
ARdur–Ad (ms)	−23.0 ± 14.7	−19.8 ± 12.3	−24.0 ± 13.6	−22.6 ± 15.8*	NS
E′-velocity (cm/s)	6.26 ± 1.18	7.03 ± 1.49†	6.19 ± 1.18	6.91 ± 1.33†	NS
E/E′ ratio	11.80 ± 2.71	12.73 ± 3.29†	11.82 ± 2.62	13.03 ± 3.20†	NS
A′-velocity (cm/s)	9.12 ± 1.42	9.20 ± 1.34	9.13 ± 1.45	9.18 ± 1.70	NS
S′-velocity (cm/s)	6.16 ± 0.93	6.29 ± 0.95	6.18 ± 0.82	6.30 ± 0.94	NS

Values are mean ± SD. The *P* values of two-sample *t*-test are shown. A-velocity, the transmitral late filling velocity; A′-velocity, tissue Doppler late diastolic velocity; ARdur–Ad, the time difference between the duration of the atrial filling wave and the duration of flow at atrial contraction; E-velocity, the transmitral early filling velocity; E′-velocity, tissue Doppler early diastolic velocity; E/E′ ratio, the ratio of early diastolic transmitral velocity to early diastolic tissue velocity; E/A ratio, the ratio of peak early to late diastolic filling velocity; EDT, the deceleration time of early diastolic filling; PLL, passive leg lifting maneuver; PVa, pulmonary vein atrial reversal; PVd, peak diastolic forward flow; PVs, peak systolic forward flow; S′-velocity, tissue Doppler systolic velocity; S/D ratio, the ratio of the pulmonary venous systolic velocity to diastolic velocity. *$P < 0.05$ and †$P < 0.01$ versus baseline.

more compromised hemodynamics, such as lower high-density lipoprotein cholesterol and eGFR, higher HOMA index, hemoglobin A1c, and LVMI. The prevalence of LVH did not significantly differ among the subgroups.

The mean time to the maximum changes occurring in the echocardiographical indices in response to PLL was 18.3 ± 3.9 s. The PLL maneuver produced a significant difference in changes in E-velocity, EDT, peak E′-velocity, and E/E′ ratio between subgroups (Table 3). The change in EDT was significantly different between subgroups (Table 3 and Figure 2a). The DM(+)/CKD(−), DM(−)/CKD(+), and DM(+)/CKD(+) groups showed a significantly greater decrease in EDT than the

Fig. 1

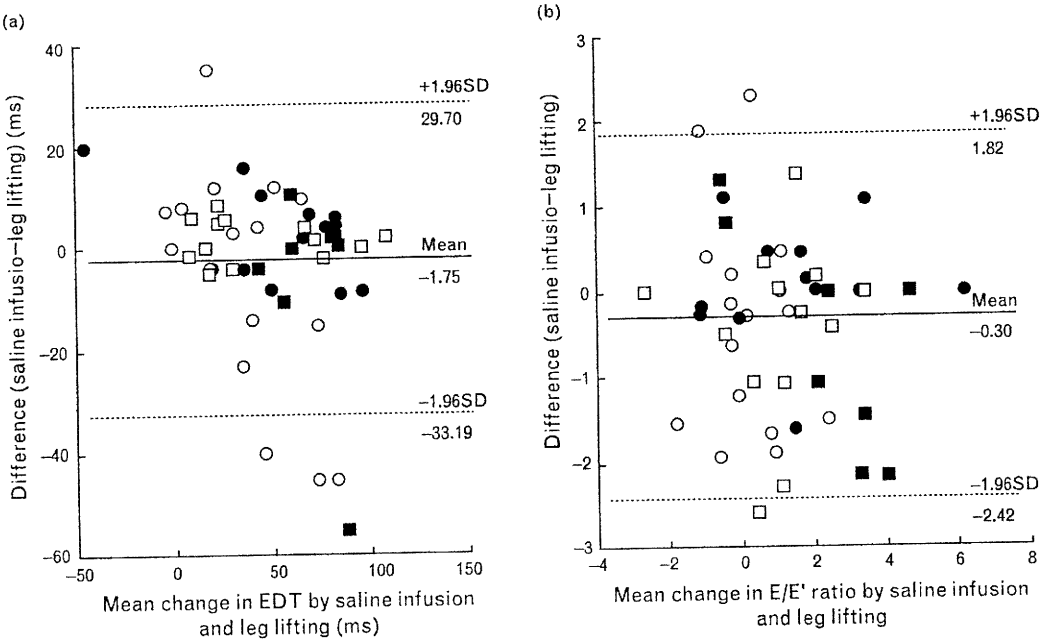

Bland–Altman plots comparing changes in echocardiographic indices by physiological saline infusion and passive leg lifting maneuver. Changes in deceleration time of early diastolic filling (EDT) (a) and the ratio of early diastolic transmitral velocity to early diastolic tissue velocity (E/E′) (b). Open circles indicate participants with diabetes mellitus (DM)(−)/CKD(−). Closed circles indicate participants with DM(+)/CKD(−). Open squares indicate participants with DM(−)/CKD(+). Closed squares indicate participants with DM(+)/CKD(+).

Table 2 Baseline clinical and hemodynamic characteristics of study participants

Variables	All	DM(−)/CKD(−)	DM(+)/CKD(−)	DM(−)/CKD(+)	DM(+)/CKD(+)	‖*P* for difference
n	155	48	25	43	39	
Age (years)	67.1 ± 8.6	66.5 ± 6.8	67.6 ± 7.5	66.6 ± 11.4	68.2 ± 7.9	NS
Male/female, *n*	100/55	27/21	12/13	32/11	29/10	<0.05
BMI (kg/m^2)	24.0 ± 3.4	23.2 ± 3.1	25.7 ± 2.8*	23.5 ± 3.5	24.6 ± 3.5	<0.05
Duration of hypertension (years)	17.8 ± 12.5	15.0 ± 11.5	13.1 ± 9.1	21.3 ± 15.0*	20.4 ± 11.0	NS
Smoking status, %						
Never/past/current	40.6/40.0/19.4	54.2/18.7§/27.1	48.0/32.0/20.0	32.6/55.8†/11.6	28.2/53.9†/17.9	<0.01
SBP (mmHg)	140.6 ± 13.8	137.9 ± 10.9	137.0 ± 12.5	143.7 ± 15.5	143.0 ± 14.2	NS
DBP (mmHg)	76.9 ± 9.5	78.9 ± 8.8	76.2 ± 10.3	76.0 ± 10.2	76.0 ± 10.3	NS
Heart rate (bpm)	65.8 ± 8.6	66.8 ± 8.4	67.4 ± 10.5	62.8 ± 7.5	66.9 ± 8.2	NS
Total cholesterol (mmol/l)	4.99 ± 0.98	4.97 ± 0.72	5.19 ± 1.13	5.15 ± 1.16	4.67 ± 0.91	NS
Triglycerides (mmol/l)	1.50 ± 0.75	1.26 ± 0.64‡	1.30 ± 0.50	1.65 ± 0.93*	1.80 ± 0.63	<0.05
HDL-chol (mmol/l)	1.21 ± 0.40	1.38 ± 0.37	1.26 ± 0.30	1.19 ± 0.49	1.01 ± 0.31†	<0.01
HOMA index	1.84 ± 2.26	1.36 ± 1.08	2.68 ± 1.87†	1.36 ± 2.16	2.41 ± 3.33†	<0.01
Hemoglobin A1c (%)	5.96 ± 1.10	5.29 ± 0.36	6.74 ± 1.22†§	5.51 ± 0.45	6.74 ± 1.30†§	<0.01
eGFR (ml/min per 1.73 m^2)	51.5 ± 28.1	75.4 ± 12.9§	73.5 ± 10.9§	31.6 ± 21.8†	30.2 ± 20.9†	<0.01
Left ventricular mass index (g/m^2)	136.4 ± 40.8	123.2 ± 30.3	127.8 ± 44.6	142.1 ± 40.5	153.7 ± 45.5†	<0.01
Left ventricular hypertrophy (%)	70.3	58.3	80.9	74.4	75.8	NS
Fractional shortening (%)	39.0 ± 6.5	39.1 ± 6.8	38.5 ± 6.7	39.8 ± 6.3	37.4 ± 6.0	NS
Therapy						
Calcium antagonist, %	71.0	54.2§	60.0	81.4†	87.2†	<0.01
β-Blocker, %	40.0	29.2§	8.0§	58.1†	53.9*	<0.01
ACE inhibitor or ARB, %	61.3	47.9	56.0	67.4	74.4	NS
Diuretic, %	30.3	16.7§	4.0§	46.5†	46.2†	<0.01

Values are mean ± SD for continuous variables, and the percentages of participants for categorical variables. ACE, angiotensin-converting enzyme inhibitor; ARB, angiotensin II receptor blocker; CKD, chronic kidney disease; DM, diabetes mellitus; eGFR, estimated glomerular filtration rate; HDL-chol, high-density lipoprotein cholesterol; HOMA index, homeostatic model assessment index. ‖The *P* values of one-way analysis of variance (ANOVA) or χ^2 test. *$P < 0.05$ and †$P < 0.01$ versus DM(−)/CKD(−). ‡$P < 0.05$ and §$P < 0.01$ versus DM(−)/CKD(+).

DM(−)/CKD(−) group. Furthermore, when compared with the DM(+)/CKD(−) group or with the DM(−)/CKD(+) group, the DM(+)/CKD(+) group showed a significantly greater decrease in EDT. Similarly, the change in E/E′ ratio was significantly different between subgroups (Table 3 and Figure 2b). E/E′ ratio did not change significantly in the DM(−)/CKD(−) group; however, a significant increase in E/E′ ratio was found in the DM(+)/CKD(−), DM(−)/CKD(+) and DM(+)/CKD(+) groups (Figure 2b). The DM(+)/CKD(−), DM(−)/CKD(+), and DM(+)/CKD(+) groups showed a significantly greater increase in E/E′ ratio than that in the DM(−)/CKD(−) group. In addition, when compared with the DM(+)/CKD(−) group or with the DM(−)/CKD(+) group, the DM(+)/CKD(+) group showed a significantly greater increase in E/E′ ratio.

During PLL, 17 of the total participants had EDT less than 150 ms. Univariate logistic regression analysis found that age, fractional shortening, baseline-EDT, DM, and CKD were significantly associated with the risk of EDT less than 150 ms during PLL (Table 4). Multiple logistic regression analysis including age, fractional shortening, and baseline-EDT was performed and revealed that DM as well as CKD was an independent predictor of EDT less than 150 ms during PLL. The further addition of antihypertensive medication to the model did not meaningfully influence the results [DM, OR: 2.09, 95% confidence interval (CI): 1.52–6.88; CKD, OR: 2.20, 95% CI: 1.21–8.50, $P < 0.05$, respectively].

During PLL, 44 of the total participants had E/E′ ratio at least 15.0. The variables that were significantly associated with the risk of E/E′ ratio at least 15.0 during PLL were age, duration of hypertension, DBP, presence of LVH, baseline-E/E′, DM, and CKD. The independent predictive value of these complications and E/E′ ratio at least 15.0 during PLL was also confirmed by multiple logistic regression analysis including age, duration of hypertension, DBP, presence of LVH, and baseline-E/E′ (Table 5). The further addition of antihypertensive medication to the model did not meaningfully influence the results (DM, OR: 4.49, 95% CI: 1.42–7.94; CKD, OR: 3.69, 95% CI: 1.39–8.45, $P < 0.05$, respectively).

Discussion

The present study demonstrated that, in hypertensive patients, the changes in echocardiographic indices by PLL maneuver showed a good correlation to those induced by physiological saline infusion. The changes in EDT as well as those in E/E′ ratio induced by PLL were significantly different between subgroups, with a joint effect that was greater than the individual effect of either disease separately. The results of multiple logistic regression analysis indicated that concomitant DM and/or CKD in hypertensive patients was an independent predictor of EDT less than 150 ms as well as E/E′ ratio at least 15.0 during PLL.

Our results were partially in accordance with previous reports that PLL resulted in increased peak E-velocity [10], shortened EDT [9,10], and increased E/A ratio [9]. Previous studies have used the PLL maneuver as a means of increasing preload. An increase in preload, produced by PLL or physiological saline infusion,

Table 3 Hemodynamics and Doppler echocardiographic indices at baseline and changes during passive leg lifting maneuver

Variables	All	DM(−)/CKD(−)	DM(+)/CKD(−)	DM(−)/CKD(+)	DM(+)/CKD(+)	*P* for difference#
SBP (mmHg)						
Baseline	140.6 ± 13.8	137.9 ± 10.9	137.0 ± 12.5	143.7 ± 15.5	143.0 ± 14.2	NS
Change from baseline	0.7 ± 1.3	0.5 ± 1.0	1.1 ± 2.1	0.3 ± 1.1	1.1 ± 1.5	NS
DBP (mmHg)						
Baseline	76.9 ± 9.5	78.9 ± 8.8	76.2 ± 10.3	76.0 ± 10.2	76.0 ± 10.3	NS
Change from baseline	1.4 ± 1.8	1.1 ± 1.3	1.0 ± 2.2	1.1 ± 2.0	1.8 ± 1.7	NS
Heart rate (bpm)						
Baseline	65.8 ± 8.6	66.8 ± 8.4	67.4 ± 10.5	62.8 ± 7.5	66.9 ± 8.2	NS
Change from baseline	1.1 ± 4.38	0.9 ± 4.1	2.2 ± 4.9	0.4 ± 7.2	1.1 ± 3.3	NS
E-velocity (m/s)						
Baseline	0.74 ± 0.17	0.68 ± 0.15†	0.73 ± 0.17	0.78 ± 0.17*	0.77 ± 0.18*	<0.05
Change from baseline	0.17 ± 0.11	0.17 ± 0.11	0.16 ± 0.11	0.13 ± 0.10	0.20 ± 0.11§	<0.01
A-velocity (m/s)						
Baseline	0.85 ± 0.19	0.78 ± 0.14	0.81 ± 0.18	0.89 ± 0.20	0.93 ± 0.21†	<0.01
Change from baseline	0.00 ± 0.09	0.01 ± 0.10	0.03 ± 0.08	−0.01 ± 0.09	0.00 ± 0.07	NS
E/A ratio						
Baseline	0.89 ± 0.22	0.89 ± 0.21	0.92 ± 0.24	0.90 ± 0.22	0.85 ± 0.24	NS
Change from baseline	0.20 ± 0.17	0.22 ± 0.17	0.18 ± 0.16	0.17 ± 0.20	0.23 ± 0.16	NS
EDT (ms)						
Baseline	246 ± 48	236 ± 41	243 ± 28	245 ± 51	264 ± 59	NS
Change from baseline	−51.1 ± 41.6	−25.2 ± 29.2§	−55.9 ± 29.7*	−48.9 ± 40.5*	−81.7 ± 42.0†§	<0.01
PVs-velocity (m/s)						
Baseline	0.63 ± 0.15	0.63 ± 0.18	0.54 ± 0.14*§	0.67 ± 0.13	0.63 ± 0.13	<0.01
Change from baseline	0.00 ± 0.10	0.02 ± 0.10	0.01 ± 0.11	−0.02 ± 0.09	−0.04 ± 0.11	NS
PVd-velocity (m/s)						
Baseline	0.41 ± 0.12	0.41 ± 0.14	0.37 ± 0.11	0.42 ± 0.10	0.40 ± 0.12	NS
Change from baseline	0.09 ± 0.11	0.07 ± 0.08	0.05 ± 0.11	0.10 ± 0.13	0.12 ± 0.13	NS
S/D ratio						
Baseline	1.62 ± 0.41	1.62 ± 0.48	1.52 ± 0.35	1.67 ± 0.39	1.64 ± 0.39	NS
Change from baseline	−0.27 ± 0.37	−0.15 ± 0.26	−0.17 ± 0.18	−0.30 ± 0.39	−0.41 ± 0.47*	NS
PVa-velocity (m/s)						
Baseline	0.28 ± 0.07	0.29 ± 0.09	0.25 ± 0.04	0.29 ± 0.07	0.28 ± 0.05	NS
Change from baseline	0.00 ± 0.04	−0.01 ± 0.06	0.01 ± 0.02	0.00 ± 0.04	0.01 ± 0.04	NS
ARdur−Ad (ms)						
Baseline	−27.9 ± 23.5	−35.2 ± 20.6	−25.8 ± 19.7	−29.7 ± 25.3	−18.2 ± 20.9	NS
Change from baseline	6.0 ± 14.4	5.7 ± 16.9	7.3 ± 8.7	5.1 ± 15.0	6.6 ± 12.5	NS
E′-velocity (cm/s)						
Baseline	6.24 ± 1.10	6.04 ± 1.04	6.10 ± 1.02	6.43 ± 1.24	6.37 ± 1.05	NS
Change from baseline	0.78 ± 1.09	1.45 ± 0.94§	0.76 ± 0.94*	0.35 ± 1.05†	0.45 ± 1.01†	<0.01
E/E′ ratio						
Baseline	12.03 ± 2.87	11.42 ± 2.30	12.14 ± 2.87	12.47 ± 3.41	12.24 ± 2.82	NS
Change from baseline	1.13 ± 2.03	0.15 ± 1.65†	1.20 ± 1.93*	1.18 ± 1.72*	2.24 ± 2.28††	<0.01
A′-velocity (cm/s)						
Baseline	8.85 ± 0.83	8.71 ± 0.80	8.96 ± 1.26	8.85 ± 0.54	8.95 ± 0.79	NS
Change from baseline	0.22 ± 0.53	0.15 ± 0.48	0.22 ± 0.45	0.21 ± 0.48	0.29 ± 0.64	NS
S′-velocity (cm/s)						
Baseline	6.21 ± 0.70	6.17 ± 0.61	6.18 ± 0.79	6.23 ± 0.79	6.25 ± 0.67	NS
Change from baseline	0.05 ± 0.60	0.06 ± 0.58	−0.04 ± 0.59	0.00 ± 0.66	0.16 ± 0.56	NS

Values are mean ± SD. A-velocity, the transmitral late filling velocity; A′-velocity, tissue Doppler late diastolic velocity; ARdur−Ad, the time difference between the duration of the atrial filling wave and the duration of flow at atrial contraction; CKD, chronic kidney disease; DM, diabetes mellitus; E-velocity, the transmitral early filling velocity; E′-velocity, tissue Doppler early diastolic velocity; E/E′ ratio, the ratio of early diastolic transmitral velocity to early diastolic tissue velocity; E/A ratio, the ratio of peak early to late diastolic filling velocity; EDT, the deceleration time of early diastolic filling; PLL, passive leg lifting maneuver; PVa, pulmonary vein atrial reversal; PVd, peak diastolic forward flow; PVs, peak systolic forward flow; S′-velocity, tissue Doppler systolic velocity; S/D ratio, the ratio of the pulmonary venous systolic velocity to diastolic velocity. #The *P* values of one-way analysis of variance (ANOVA) are shown. *$P < 0.05$ and †$P < 0.01$ versus DM(−)/CKD(−). ‡$P < 0.05$ and §$P < 0.01$ versus DM(−)/CKD(+).

increases the driving pressure at mitral valve opening, resulting in an increase in peak E-velocity because of higher left atrial pressure on mitral valve opening and decreased EDT in parallel with a decline in left ventricular compliance. E′-velocity was determined by left ventricular relaxation, minimal pressure, and preload [27], and E/E′ ratio was modulated by increased preload induced by PLL. In accordance with previous findings [9,10], blood pressure as well as heart rate remained statistically unchanged, and thus, the results of our comparative study confirmed the clinical utility of the PLL maneuver as a means of increasing preload without altering afterload.

EDT is dependent on the rate of increase in left ventricular pressure in early diastole, after it has reached its nadir, and is a measure of the effective operative chamber compliance of the left ventricle [6,28,29]. Because the mitral inflow velocity profile is affected by several factors, including suction, volume status, left atrial pressure, and rate of myocardial relaxation [6,7,30], we also performed tissue Doppler imaging of mitral annular motion. E′-velocity is a less preload-dependent index of early left ventricular relaxation than conventional Doppler parameters, and it has also been validated against the Tau index [31], the time constant of isovolumic relaxation. Nevertheless, E′-velocity was also dependent on

Fig. 2

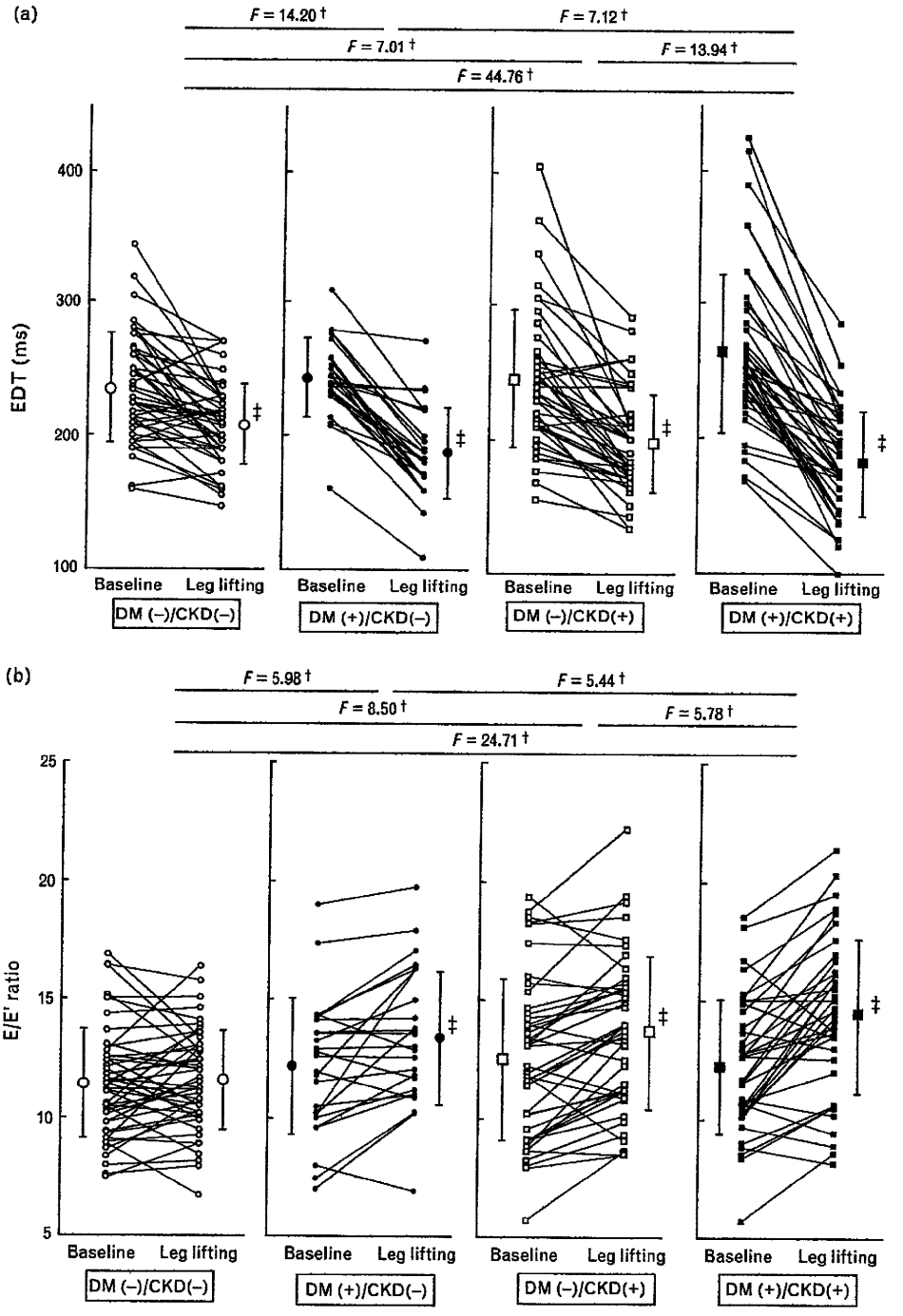

Changes in deceleration time of early diastolic filling (EDT) (a) ($F = 15.92$, $P_{trend} < 0.01$) and the ratio of early diastolic transmitral velocity to early diastolic tissue velocity (E/E') (b) ($F = 8.87$, $P_{trend} < 0.01$) by passive leg lifting (PLL) maneuver. Data are presented as individual plots and means ± SD. CKD, chronic kidney disease; DM, diabetes mellitus. $^{*}P < 0.05$ and $^{\dagger}P < 0.01$. $^{\ddagger}P < 0.01$ versus baseline.

Table 4 Predictors of EDT less than 150 ms during PLL by crude and multivariate logistic regression analysis

Variables, unit of increase	Crude		Multivariate adjusted	
	OR (95% CI)	*P*	OR (95% CI)	*P*
Age, 1 year	1.08 (1.01–1.16)	<0.05	1.10 (0.98–1.23)	NS
Fractional shortening, 1%	0.89 (0.80–0.98)	<0.01	0.88 (0.76–1.02)	NS
Baseline EDT, 1 ms	0.97 (0.95–0.98)	<0.01	0.94 (0.91–0.97)	<0.01
DM, yes	3.97 (1.32–11.91)	<0.01	2.82 (1.03–7.67)	<0.05
CKD, yes	3.25 (1.01–10.46)	<0.01	2.18 (1.18–8.44)	<0.05

Values are odds ratio [95% confidence interval (CI)]. CKD, chronic kidney disease; DM, diabetes mellitus; EDT, the deceleration time of early diastolic filling; NS, not significant; PLL, passive leg lifting.

preload modulation [27,32], and combining transmitral flow velocity with annular velocity (E/E′ ratio) has been proposed as a tool for assessing left ventricular filling pressures that combines the influence of transmitral driving pressure and myocardial relaxation [33–36]. Previous studies in healthy individuals found that the E/E′ ratio did not change significantly in response to PLL [10] or physiological saline infusion [37]. In contrast, the hemodialysis-related volume reduction produced a significant decrease in E/E′ ratio [38]. Our results found that EDT and E/E′ ratio at baseline were not significantly different among subgroups; however, the changes in EDT as well as those in E/E′ ratio showed a stepwise increase in hypertensive patients with complications such as DM and/or CKD. E/E′ ratio did not change significantly in the subgroup without complications; however, a significant increase in E/E′ ratio was found in the subgroups with complications. In addition, in hypertensive patients, concomitant DM and/or CKD was independently associated with EDT less than 150 ms as well as E/E′ ratio at least 15.0 during PLL, which were proven cut-off values to predict decreased left ventricular stiffness [28,36,39], suggesting that different degrees of latent diastolic dysfunction and preload reserve may account for the divergent response of EDT as well as E/E′ ratio to PLL. Patients with reduced compliance may not have the ability to alter their filling pattern in response to an increase in preload, depending on left ventricular operating chamber compliance, and those with less compliant ventricles are much more sensitive to alterations in filling volume, with a marked increase in filling pressure with a relatively small increase in volume [6,40]. These Doppler changes may result from the development of elevated filling pressures and from accelerated relaxation occurring as a consequence of increased contractility. The baseline Doppler indices and their changes after loading manipulations may represent several steps of left ventricular remodeling, and a decreased response to increased preload may predispose to the development of more severe abnormal left ventricular relaxation. Thus, one novel aspect of this study is the demonstration that hypertensive patients with DM and/or CKD have reduced left ventricular compliance and preload reserve. The results from the Strong Heart Study indicated that concomitant DM further adds to the impairment of left ventricular relaxation associated with hypertension [14]. Left ventricular stiffness, which modulates left ventricular diastolic function, is modulated by changes in the extracellular matrix (collagen accumulation), shifts in titin, and endothelial dysfunction. Previous studies support the view that the diabetic state *per se* affects left ventricular dysfunction, due to decreased vessel wall content of heparin sulfate [41], interstitial accumulation of advanced-glycated end products [42,43], and other factors [44,45]. In CKD, factors in the pathogenesis of myocardial fibrosis include acidosis, slower calcium uptake, angiotensin II, chronically elevated parathyroid hormone, endothelin, aldosterone, and increased plasma catecholamines [46]. In addition, a significantly higher LVMI, which has been implicated in the pathogenesis of left ventricular diastolic dysfunction, was observed in the DM(+)/CKD(+) group, and thus LVH could be one of the possible mechanisms of

Table 5 Predictors of the ratio of E/E′ ratio at least 15.0 during PLL by crude and multivariate logistic regression analysis

Variables, unit of increase	Crude		Multivariate adjusted	
	OR (95% CI)	*P*	OR (95% CI)	*P*
Age, 1 year	1.22 (1.13–1.32)	<0.01	1.29 (1.13–1.48)	<0.01
Duration of hypertension, 1 year	1.05 (1.03–1.08)	<0.01	0.98 (0.92–1.03)	NS
DBP, 1 mmHg	0.92 (0.88–0.96)	<0.01	0.99 (0.91–1.08)	NS
Left ventricular hypertrophy, yes	2.98 (1.22–7.30)	<0.05	0.90 (0.18–4.37)	NS
Baseline-E/E′, 1 unit	1.86 (1.53–2.34)	<0.01	3.00 (1.84–4.90)	<0.01
DM, yes	2.43 (1.19–4.95)	<0.01	4.78 (1.84–8.60)	<0.05
CKD, yes	4.46 (2.01–9.92)	<0.01	3.32 (1.48–8.92)	<0.05

Values are odds ratio (95% CI). CI, confidence interval; CKD, chronic kidney disease; DBP, diastolic blood pressure; DM, diabetes mellitus; E/E′, the ratio of transmitral early left ventricular filling velocity to early diastolic Doppler tissue imaging of the mitral annulus.

our results. Previous reports showed that hypertension with complications such as DM or CKD was associated with increased risk of CVD [1–5], and our results may support investigation of the mechanisms of cardiovascular disorders in hypertensive patients with complications.

It must be emphasized that no 'cut-off' values were provided based on the results of this study. Despite the significant difference in the change in EDT as well as that in E/E′ ratio during PLL between hypertensive patients with/without DM and/or CKD, overlap was present. Other investigators have used the criterion of a baseline 'E/A ratio less than 1.0 (whatever the value of EDT)', becoming 'E/A ratio more than 1.0 and EDT of 130 or less' during the PLL maneuver [8,9]. However, this criterion could not be applied to our patients because only a few patients had a decrease in EDT to 130 or less during PLL. Mitral flow pattern is usually assessed only once, at baseline, and this may be a limitation because it may change spontaneously in some patients. Accordingly, we hypothesized that changes in Doppler echocardiographic indices in response to loading manipulations such as PLL could provide an estimate of cardiovascular reserve and add information on latent diastolic dysfunction. Previous studies have confirmed the validity of this maneuver in patients with chronic heart failure [8,9]; however, the prognostic value of this maneuver in hypertensive patients remains to be elucidated. Therefore, this study should be viewed as a preliminary investigation to support future studies to determine the ultimate clinical utility of this maneuver.

In hypertensive patients, the PLL maneuver is a useful procedure as a means of increasing preload and could be useful to estimate the effective operative left ventricular compliance. Concomitant DM and/or CKD was independently associated with an exaggerated change in EDT as well as change in E/E′ ratio in response to the PLL maneuver. Our results suggest that this simple preloading test may unmask the latent progression of left ventricular dysfunction; that is, these complications potentially cause deterioration of left ventricular compliance and preload reserve even in the early stages of diastolic dysfunction. The present findings may support investigation of the actual mechanisms of the increased CVD risk in hypertensive patients with DM or CKD. These findings need to be confirmed in larger prospective studies investigating the importance of early detection and treatment of latent diastolic dysfunction in hypertension, which may be an important risk factor for heart failure as well as CVD.

References

1 Jarrett RJ, McCartney P, Keen H. The Bedford survey: ten year mortality rates in newly diagnosed diabetics, borderline diabetics and normoglycaemic controls and risk indices for coronary heart disease in borderline diabetics. *Diabetologia* 1982; **22**:79–84.

2 Shulman NB, Ford CE, Hall WD, Blaufox MD, Simon D, Langford HG, Schneider KA. Prognostic value of serum creatinine and effect of treatment of hypertension on renal function. Results from the hypertension detection and follow-up program. The Hypertension Detection and Follow-up Program Cooperative Group. *Hypertension* 1989; **13**:180–193.

3 Samuelsson O, Wilhelmsen L, Elmfeldt D, Pennert K, Wedel H, Wikstrand J, Berglund G. Predictors of cardiovascular morbidity in treated hypertension: results from the primary preventive trial in Goteborg, Sweden. *J Hypertens* 1985; **3**:167–176.

4 Ruilope LM, Salvetti A, Jamerson K, Hansson L, Warnold I, Wedel H, Zanchetti A. Renal function and intensive lowering of blood pressure in hypertensive participants of the Hypertension Optimal Treatment (HOT) study. *J Am Soc Nephrol* 2001; **12**:218–225.

5 Verdecchia P, Reboldi G, Angeli F, Borgioni C, Gattobigio R, Filippucci L, *et al.* Adverse prognostic significance of new diabetes in treated hypertensive subjects. *Hypertension* 2004; **43**:963–969.

6 Nishimura RA, Tajik AJ. Evaluation of diastolic filling of left ventricle in health and disease: Doppler echocardiography is the clinician's Rosetta Stone. *J Am Coll Cardiol* 1997; **30**:8–18.

7 Choong CY, Herrmann HC, Weyman AE, Fifer MA. Preload dependence of Doppler-derived indexes of left ventricular diastolic function in humans. *J Am Coll Cardiol* 1987; **10**:800–808.

8 Capomolla S, Pinna GD, Febo O, Caporotondi A, Guazzotti G, La Rovere MT, *et al.* Echo-Doppler mitral flow monitoring: an operative tool to evaluate day-to-day tolerance to and effectiveness of beta-adrenergic blocking agent therapy in patients with chronic heart failure. *J Am Coll Cardiol* 2001; **38**:1675–1684.

9 Pozzoli M, Traversi E, Cioffi G, Stenner R, Sanarico M, Tavazzi L. Loading manipulations improve the prognostic value of Doppler evaluation of mitral flow in patients with chronic heart failure. *Circulation* 1997; **95**:1222–1230.

10 Paelinck BP, van Eck JW, De Hert SG, Gillebert TC. Effects of postural changes on cardiac function in healthy subjects. *Eur J Echocardiogr* 2003; **4**:196–201.

11 Shimizu Y, Uematsu M, Shimizu H, Nakamura K, Yamagishi M, Miyatake K. Peak negative myocardial velocity gradient in early diastole as a noninvasive indicator of left ventricular diastolic function: comparison with transmitral flow velocity indices. *J Am Coll Cardiol* 1998; **32**:1418–1425.

12 De Hert SG, Gillebert TC, Ten Broecke PW, Moulijn AC. Length-dependent regulation of left ventricular function in coronary surgery patients. *Anesthesiology* 1999; **91**:379–387.

13 Wachtell K, Smith G, Gerdts E, Dahlof B, Nieminen MS, Papademetriou V, *et al.* Left ventricular filling patterns in patients with systemic hypertension and left ventricular hypertrophy (the LIFE study). Losartan Intervention For Endpoint. *Am J Cardiol* 2000; **85**:466–472.

14 Liu JE, Palmieri V, Roman MJ, Bella JN, Fabsitz R, Howard BV, *et al.* The impact of diabetes on left ventricular filling pattern in normotensive and hypertensive adults: the Strong Heart Study. *J Am Coll Cardiol* 2001; **37**:1943–1949.

15 Liu JE, Robbins DC, Palmieri V, Bella JN, Roman MJ, Fabsitz R, *et al.* Association of albuminuria with systolic and diastolic left ventricular dysfunction in type 2 diabetes: the Strong Heart Study. *J Am Coll Cardiol* 2003; **41**:2022–2028.

16 Fathi R, Isbel N, Haluska B, Case C, Johnson DW, Marwick TH. Correlates of subclinical left ventricular dysfunction in ESRD. *Am J Kidney Dis* 2003; **41**:1016–1025.

17 Expert Committee on the Diagnosis and Classification of Diabetes Mellitus. Report of the expert committee on the diagnosis and classification of diabetes mellitus. *Diabetes Care* 2003; **26 (Suppl 1)**: S5–S20.

18 National Kidney Foundation. K/DOQI clinical practice guidelines for chronic kidney disease: evaluation, classification, and stratification. *Am J Kidney Dis* 2002; **39**:S1–S266.

19 Iwashima Y, Horio T, Kamide K, Rakugi H, Ogihara T, Kawano Y. Uric acid, left ventricular mass index, and risk of cardiovascular disease in essential hypertension. *Hypertension* 2006; **47**:195–202.

20 Iwashima Y, Horio T, Kamide K, Rakugi H, Ogihara T, Kawano Y. Pulmonary venous flow and risk of cardiovascular disease in essential hypertension. *J Hypertens* 2008; **26**:798–805.

21 Lang RM, Bierig M, Devereux RB, Flachskampf FA, Foster E, Pellikka PA, *et al.* Recommendations for chamber quantification: a report from the American Society of Echocardiography's Guidelines and Standards Committee and the Chamber Quantification Writing Group, developed in conjunction with the European Association of Echocardiography, a branch of the European Society of Cardiology. *J Am Soc Echocardiogr* 2005; **18**:1440–1463.

22 Cooper JW, Nanda NC, Philpot EF, Fan P. Evaluation of valvular regurgitation by color Doppler. *J Am Soc Echocardiogr* 1989; **2**:56–66.

23 Devereux RB, Alonso DR, Lutas EM, Gottlieb GJ, Campo E, Sachs I, Reichek N. Echocardiographic assessment of left ventricular hypertrophy: comparison to necropsy findings. *Am J Cardiol* 1986; **57**:450–458.

24 Ghali JK, Liao Y, Simmons B, Castaner A, Cao G, Cooper RS. The prognostic role of left ventricular hypertrophy in patients with or without coronary artery disease. *Ann Intern Med* 1992; **117**:831–836.

25 Devereux RB, Dahlof B, Levy D, Pfeffer MA. Comparison of enalapril versus nifedipine to decrease left ventricular hypertrophy in systemic hypertension (the PRESERVE trial). *Am J Cardiol* 1996; **78**:61–65.

26 Basnight MA, Gonzalez MS, Kershenovich SC, Appleton CP. Pulmonary venous flow velocity: relation to hemodynamics, mitral flow velocity and left atrial volume, and ejection fraction. *J Am Soc Echocardiogr* 1991; **4**:547–558.

27 Nagueh SF, Sun H, Kopelen HA, Middleton KJ, Khoury DS. Hemodynamic determinants of the mitral annulus diastolic velocities by tissue Doppler. *J Am Coll Cardiol* 2001; **37**:278–285.

28 Little WC, Ohno M, Kitzman DW, Thomas JD, Cheng CP. Determination of left ventricular chamber stiffness from the time for deceleration of early left ventricular filling. *Circulation* 1995; **92**:1933–1939.

29 Ohno M, Cheng CP, Little WC. Mechanism of altered patterns of left ventricular filling during the development of congestive heart failure. *Circulation* 1994; **89**:2241–2250.

30 Kuo LC, Quinones MA, Rokey R, Sartori M, Abinader EG, Zoghbi WA. Quantification of atrial contribution to left ventricular filling by pulsed Doppler echocardiography and the effect of age in normal and diseased hearts. *Am J Cardiol* 1987; **59**:1174–1178.

31 Sohn DW, Chai IH, Lee DJ, Kim HC, Kim HS, Oh BH, *et al.* Assessment of mitral annulus velocity by Doppler tissue imaging in the evaluation of left ventricular diastolic function. *J Am Coll Cardiol* 1997; **30**:474–480.

32 Firstenberg MS, Greenberg NL, Main ML, Drinko JK, Odabashian JA, Thomas JD, Garcia MJ. Determinants of diastolic myocardial tissue Doppler velocities: influences of relaxation and preload. *J Appl Physiol* 2001; **90**:299–307.

33 Nagueh SF, Lakkis NM, Middleton KJ, Spencer WH 3rd, Zoghbi WA, Quinones MA. Doppler estimation of left ventricular filling pressures in patients with hypertrophic cardiomyopathy. *Circulation* 1999; **99**:254–261.

34 Nagueh SF, Middleton KJ, Kopelen HA, Zoghbi WA, Quinones MA. Doppler tissue imaging: a noninvasive technique for evaluation of left ventricular relaxation and estimation of filling pressures. *J Am Coll Cardiol* 1997; **30**:1527–1533.

35 Nagueh SF, Mikati I, Kopelen HA, Middleton KJ, Quinones MA, Zoghbi WA. Doppler estimation of left ventricular filling pressure in sinus tachycardia. A new application of tissue doppler imaging. *Circulation* 1998; **98**:1644–1650.

36 Ommen SR, Nishimura RA, Appleton CP, Miller FA, Oh JK, Redfield MM, Tajik AJ. Clinical utility of Doppler echocardiography and tissue Doppler imaging in the estimation of left ventricular filling pressures: a comparative simultaneous Doppler-catheterization study. *Circulation* 2000; **102**:1788–1794.

37 Firstenberg MS, Levine BD, Garcia MJ, Greenberg NL, Cardon L, Morehead AJ, *et al.* Relationship of echocardiographic indices to pulmonary capillary wedge pressures in healthy volunteers. *J Am Coll Cardiol* 2000; **36**:1664–1669.

38 Hung KC, Huang HL, Chu CM, Chen CC, Hsieh IC, Chang ST, *et al.* Evaluating preload dependence of a novel Doppler application in assessment of left ventricular diastolic function during hemodialysis. *Am J Kidney Dis* 2004; **43**:1040–1046.

39 Yong Y, Nagueh SF, Shimoni S, Shan K, He ZX, Reardon MJ, *et al.* Deceleration time in ischemic cardiomyopathy: relation to echocardiographic and scintigraphic indices of myocardial viability and functional recovery after revascularization. *Circulation* 2001; **103**:1232–1237.

40 Khouri SJ, Maly GT, Suh DD, Walsh TE. A practical approach to the echocardiographic evaluation of diastolic function. *J Am Soc Echocardiogr* 2004; **17**:290–297.

41 Deckert T, Feldt-Rasmussen B, Borch-Johnsen K, Jensen T, Kofoed-Enevoldsen A. Albuminuria reflects widespread vascular damage. The Steno hypothesis. *Diabetologia* 1989; **32**:219–226.

42 Regan TJ, Lyons MM, Ahmed SS, Levinson GE, Oldewurtel HA, Ahmad MR, Haider B. Evidence for cardiomyopathy in familial diabetes mellitus. *J Clin Invest* 1977; **60**:884–899.

43 van Hoeven KH, Factor SM. A comparison of the pathological spectrum of hypertensive, diabetic, and hypertensive-diabetic heart disease. *Circulation* 1990; **82**:848–855.

44 Flarsheim CE, Grupp IL, Matlib MA. Mitochondrial dysfunction accompanies diastolic dysfunction in diabetic rat heart. *Am J Physiol* 1996; **271**:H192–202.

45 Schaffer SW, Mozaffari MS, Artman M, Wilson GL. Basis for myocardial mechanical defects associated with noninsulin-dependent diabetes. *Am J Physiol* 1989; **256**:E25–30.

46 London GM. Left ventricular alterations and end-stage renal disease. *Nephrol Dial Transplant* 2002; **17 (Suppl 1)**:29–36.

Hypertension Research (2010) 33, 1244–1249

www.nature.com/hr

ORIGINAL ARTICLE

Impact of RGS2 deficiency on the therapeutic effect of telmisartan in angiotensin II-induced aortic aneurysm

Sachiko Matsumoto[1], Kei Kamide[1,2], Fumiaki Banno[1], Nobutaka Inoue[1,3], Naoki Mochizuki[1], Yuhei Kawano[4] and Toshiyuki Miyata[1]

Regulator of G-protein signaling 2 (RGS2) negatively regulates the signaling of G-protein-coupled receptors, such as the angiotensin II (AngII) type 1 receptor by accelerating the inactivation of Gαq. Rgs2-deficient mice show increased sensitivity and prolonged responsiveness to vasoconstrictors, and genetic variations in the *RGS2* gene are associated with hypertension in humans. This study aimed to clarify whether Rgs2 deficiency contributes to the development of vascular remodeling and therapeutic efficacy of the angiotensin receptor blocker telmisartan on atherosclerotic vascular damage. We treated *Rgs2*$^{+/+}$, *Rgs2*$^{+/-}$ and *Rgs2*$^{-/-}$ mice with saline (control group), AngII (1000 ng per kg per min, AngII group) or low-dose telmisartan (0.3 mg per kg per day) with AngII infusion (AngII+Telmi group) for 4 weeks. For all genotypes, the AngII groups exhibited significantly higher blood pressure, a higher mortality rate and a higher incidence of aortic aneurysm than the respective control group. Interestingly, aneurysm incidence was decreased in the AngII+Telmi group compared with the AngII group in *Rgs2*$^{-/-}$ mice (6.7 *vs.* 42.9%, $P<0.05$), but not in *Rgs2*$^{+/+}$ mice (38.9 *vs.* 40.0%). Moreover, in *Rgs2*$^{-/-}$ mice, the AngII+Telmi group exhibited significant improvement in survival, reduction of enlarged aortic diameter, inhibition of superoxide production and suppression of NAD(P)H oxidase activity compared with the AngII group. Thus, Rgs2 deficiency potentiates the vascular protection effect of low-dose telmisartan. Our results suggest that angiotensin receptor blocker may be useful for protection from cardiovascular events in hypertensive subjects with risk alleles in the *RGS2* gene.
Hypertension Research (2010) **33**, 1244–1249; doi:10.1038/hr.2010.184; published online 30 September 2010

Keywords: angiotensin II; aortic aneurysm; oxidative stress; RGS2; telmisartan

INTRODUCTION

The renin–angiotensin system has an important role in the regulation of blood pressure and vascular structure. Angiotensin II (AngII) is a potent vasoconstrictor that elevates blood pressure through a G-protein-coupled receptor, angiotensin type 1 receptor (AT1R). AngII generates aldosterone at the adrenal gland and activates the sympathetic nervous system, leading to blood pressure elevation. In addition to the effects of AngII on the elevation of blood pressure, evidence has revealed that it has a role in atherogenesis. In animal models, chronic infusion of AngII promotes the formation of atherosclerotic lesions and aneurysms.[1,2] It is widely known that AngII-induced NAD(P)H oxidase activation increases the production of reactive oxygen species from various cell types,[3] including endothelial cells, vascular smooth muscle cells and monocytes/macropharges, and promotes inflammation in atherosclerotic lesions.[4]

Regulator of G-protein signaling 2 (RGS2) is present in many cardiovascular tissues, including the heart, kidney and blood vessels, and it is required for normal vascular function and regulation of blood pressure.[5] RGS2 negatively regulates the signaling of G-protein-coupled receptors, such as AT_1R, by accelerating the inactivation of Gαq by its guanosine triphosphatase-activating protein activity. RGS2 also mediates the nitric oxide–cyclic guanosine monophosphate pathway to decrease vascular resistance and attenuate vasoconstrictor signaling in vascular smooth muscle cells.[5,6] Patients with Bartter's and Gitelman's syndromes have hypotension with an enhancement of RGS2 expression.[7] Taken together, silencing of the *RGS2* gene disrupts these pathways and enhances the vasoconstrictor signaling.

The first reported phenotypes of Rgs2-deficient mice were the reduction of T-cell activation, the control of synapse development in the hippocampus and an increase in anxiety responses.[8] With respect to the blood pressure regulation, Rgs2-deficient mice exhibit a hypertensive phenotype and persistent constriction of the resistance vasculature.[5,9] This hypertensive phenotype differs in degree according to conditions such as age in weeks, anesthesia, postoperative recovery, restrained stress, time zone and apparatus for blood pressure measurement.[5,9,10] Together with another group, we have reported that genetic polymorphisms within the human *RGS2* gene are associated with hypertension.[11–14] It has been speculated that genetic variations

[1]Research Institute, National Cerebral and Cardiovascular Center, Suita, Osaka, Japan; [2]Department of Geriatric Medicine and Nephrology, Osaka University Graduate School of Medicine, Suita, Osaka, Japan; [3]Department of Cardiovascular Medicine, Kobe Rosai Hospital, Kobe, Hyogo, Japan and [4]Division of Hypertension and Nephrology, National Cerebral and Cardiovascular Center, Suita, Osaka, Japan
Correspondence: Dr K Kamide, Department of Geriatric Medicine and Nephrology, Osaka University Graduate School of Medicine, 2-2, Yamadaoka, Suita city, Osaka 565-0871, Japan.
E-mail: kamide@geriat.med.osaka-u.ac.jp
Received 28 May 2010; revised 21 June 2010; accepted 28 June 2010; published online 30 September 2010

may reduce RGS2 function.[15,16] Because hypertension contributes to the pathogenesis of cardiovascular disease, it is hypothesized that genetic variations in RGS2 might be a risk factor for the development of atherosclerosis through enhancement of AngII signaling.

Telmisartan is an angiotensin receptor blocker (ARB) with a longer half-life and higher lipophilicity than other ARBs,[17] and it is a commonly used medication for the treatment of hypertension. In a recent clinical trial,[18,19] telmisartan resulted in the prevention of vascular events such as myocardial infarction and stroke. Therefore, telmisartan is expected to be effective for cardiovascular protection in Rgs2-deficient mice that have enhanced AngII signaling.

In this study, we investigated the effects of RGS2 deficiency on the development of vascular remodeling and the therapeutic efficacy of low-dose telmisartan on atherosclerotic vascular damage resulting from excessive stimulation of AT_1R by RGS2 deficiency.

METHODS

Mice

Rgs2-deficient mice on the C57BL/6 background were provided by Dr Michael E Mendelsohn (Tufts University School of Medicine).[8] Mice were kept in a specific pathogen-free barrier under constant temperature conditions and housed on a 12-h light/12 h dark cycle. All experiments were approved by the Animal Care and Use Committees of the National Cardiovascular Center, Japan, and they were performed in accordance with the guidelines.

Drug administration

We used 18-week old male Rgs2-deficient ($Rgs2^{-/-}$, $Rgs2^{+/-}$) and wild-type ($Rgs2^{+/+}$) mice and divided them into three treatment groups. Mice were subcutaneously infused with AngII (1000 ng per kg per min, AngII group), or saline containing 0.3% bovine serum albumin (control group) using an ALZET Micro-Osmotic Pump (model 1004, Durect, Cupertino, CA, USA) for 4 weeks. Mice were also treated with AngII (1000 ng per kg per min) and low-dose telmisartan (0.3 mg per kg per day, AngII+Telmi group). Telmisartan was administered in drinking water. We adopted a low dosage of telmisartan that does not affect blood pressure.[20]

Hemodynamic analysis

Systolic blood pressure and heart rate were measured in conscious, pre-warmed, and restrained mice by the tail-cuff method using a non-invasive blood pressure measuring device (BP98-A, Softron, Tokyo, Japan) before treatment and on days 7, 14, 21 and 28 after treatment just around the same time of day. For stable measurement, tail-cuff pressures were obtained after a 2-week-training period to acclimatize the mice to the restraining device and cuff inflation. The pulse waveform was monitored in real time using the BP98AW software (version 2.12, Softron). The first 10 measurements were excluded from the analysis, and at least 5 measurements with an untroubled pulse waveform were collected.

Biochemical examination

After 4 weeks of treatment, overnight fasting blood was collected from anesthetized mice and put into capillary blood collection tubes including a gel/clot activator (Capiject tube, Terumo Medical, Somerset, NJ, USA). Serum was obtained by the manufacturer's instructions and stored at −80 °C in aliquots before use. Serum levels of blood urea nitrogen, creatinine, aspartate aminotransferase, alanine aminotransferase, lactate dehydrogenase, low-density lipoprotein-cholesterol and glucose were measured using a Hitachi clinical analyzer (model 7180, Hitachi High-Technologies, Tokyo, Japan).

Aortic tissue collection and morphometric analysis

Dissection was performed under anesthesia after blood collection. After thoracolaparotomy, the inferior vena cava was cut for exsanguination and the aorta was perfused with ice-cold saline through the left ventricle. The aortic root and heart were subsequently eviscerated, and the periadventitial tissue was dissected away under a stereomicroscope. The external diameters in the middle of the suprarenal abdominal aorta between the diaphragm and renal artery bifurcation were measured using the ImageJ software (version 1.40, National Institute of Health, Bethesda, MD, USA). After taking the images, the aorta was cut into thoracic and abdominal regions. The thoracic aorta was immediately frozen by liquid nitrogen and stored at −80 °C for the measurement of NAD(P)H oxidase activity. The suprarenal abdominal aorta was cut into two pieces. For detection of superoxide production, the superior half was immediately embedded in OCT compound (Sakura Finetek Japan, Tokyo, Japan) in liquid nitrogen and stored at −80 °C. For immunohistochemical staining, the inferior half was fixed with 4% paraformaldehyde overnight and paraffin embedded.

Detection of aortic superoxide production

Aortic superoxide levels were measured with dihydroethidium (Invitrogen Molecular Probes, Carlsbad, CA, USA) on cross sections (9 μm) obtained from the unfixed frozen blocks of abdominal aorta, as previously described.[21] The unfixed frozen sections were stained by dihydroethidium (2 μM, 30 min, 37 °C) in a dark humidified chamber and washed briefly. The images were captured with a laser scanning confocal fluorescent microscope (FLUOVIEW system, Olympus, Tokyo, Japan). For the quantification of ethidium fluorescence, the mean fluorescence intensity (fluorescence intensity per unit area) in the aortic wall was calculated using the ImageJ software on high-power (x300) images.

Measurement of NAD(P)H oxidase activity

The frozen aortic segments were homogenized using a Sample Grinding Kit (GE Healthcare UK, Buckinghamshire, England). After centrifugation, the supernatant was stored at −80 °C until use. Protein concentrations were measured by the BCA protein assay kit (Pierce Biotechnology, Rockford, IL, USA). The enzymatic activity of NAD(P)H oxidase of the homogenates was measured by lucigenin-enhanced chemiluminescence, as previously described.[20] The assay solution contained lucigenin (250 μM) as an electron acceptor and NADH (100 μM) or NADPH (100 μM) as a substrate. After pre-incubation at 37 °C for 20 min, the reaction was started by adding 50 μg of homogenate. Photon emissions were continuously recorded for 15 min with a chemiluminescence reader (BLR-201, ALOKA, Tokyo, Japan). The chemiluminescent signals observed in the absence of homogenates were subtracted from the signals of the samples. The signal was corrected for the protein concentration of each homogenate and expressed as counts per minute by mg protein for a 15-min period. In some experiments, the homogenates were pre-incubated with 10 μM diphenyleneiodium, a selective NADPH oxidase inhibitor, for 20 min before the lucigenin-enhanced chemiluminescence measurements.

Statistical analysis

Data are expressed as mean ± s.e.m. All statistical analyses were performed using the Prism software (version 5.0, GraphPad Software, La Jolla, CA, USA). Hemodynamic changes were analyzed by two-way analysis of variance during the period of administration. Differences between multiple groups were analyzed by one-way analysis of variance or Kruskal–Wallis test in the case of a non-Gaussian distribution, followed by the Bonferroni *post-hoc* test for comparison between treatment groups or genotype groups. The log-rank (Mantel–Cox) test was used for statistical analysis of survival curves, and the χ^2-test was used to compare the incidence of aneurysm. Values of $P<0.05$ were considered statistically significant.

RESULTS

Changes in blood pressure

To elucidate the direct role of AngII signaling in Rgs2-deficient mice, we divided $Rgs2^{+/+}$, $Rgs2^{+/-}$ and $Rgs2^{-/-}$ mice into three treatment groups: the control group, the AngII group and the AngII+Telmi group. Drug administration was performed for 4 weeks, and hemodynamic changes were measured. In all Rgs2 genotypes, the AngII group exhibited ~50 mm Hg higher systolic blood pressure than the control group ($P<0.001$) (Figure 1). Rgs2 dysfunction was expected to enhance the AngII signaling, leading to higher blood pressure in

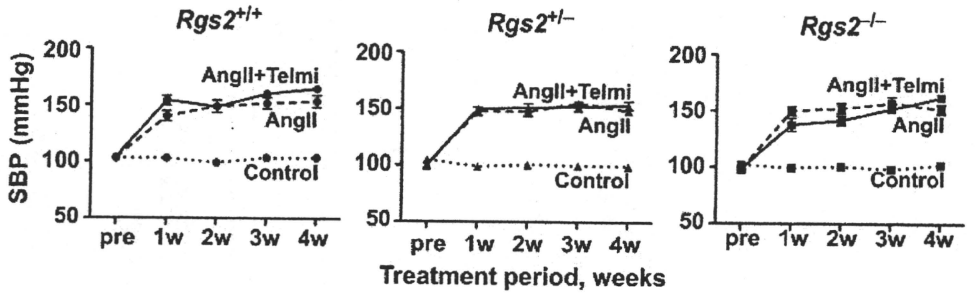

Figure 1 Blood pressure changes in response to AngII or AngII plus telmisartan. Systolic blood pressure (SBP) variations were shown in *Rgs2*$^{+/+}$, *Rgs2*$^{+/-}$ and *Rgs2*$^{-/-}$ mice. Mice were divided into three groups, control group (saline), AngII group (AngII, 1000 ng per kg per min) and AngII+Telmi group (AngII, 1000 ng per kg per min, telmisartan, 0.3 mg per kg per day). Results are expressed as mean ± s.e.m. in the control group (*Rgs2*$^{+/+}$: n=8, *Rgs2*$^{+/-}$: n=8, *Rgs2*$^{-/-}$: n=8), the AngII group (*Rgs2*$^{+/+}$: n=17, *Rgs2*$^{+/-}$: n=25, *Rgs2*$^{-/-}$: n=15) and the AngII+Telmi group (*Rgs2*$^{+/+}$: n=14, *Rgs2*$^{+/-}$: n=15, *Rgs2*$^{-/-}$: n=15). The AngII and AngII+Telmi groups showed significantly higher SBP than the control group (P<0.001).

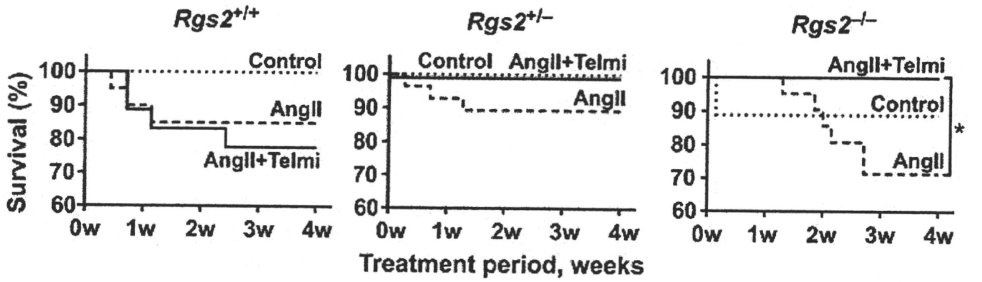

Figure 2 Comparison of survival curves in mice treated with AngII or AngII plus telmisartan. The treatment design was the same as that in Figure 1. The survival rate is expressed as a percent of animals in the control group (*Rgs2*$^{+/+}$: n=8, *Rgs2*$^{+/-}$: n=8, *Rgs2*$^{-/-}$: n=9), the AngII group (*Rgs2*$^{+/+}$: n=20, *Rgs2*$^{+/-}$: n=28, *Rgs2*$^{-/-}$: n=21) and the AngII+Telmi group (*Rgs2*$^{+/+}$: n=18, *Rgs2*$^{+/-}$: n=15, *Rgs2*$^{-/-}$: n=15). *P<0.05.

Rgs2$^{-/-}$ mice, but there were no blood pressure differences among the Rgs2 genotypes in the AngII group. Moreover, the AngII+Telmi group did not show reduced blood pressure in any of the genotypes. Before drug administration, there were no significant differences in blood pressure among the Rgs2 genotypes in our experimental condition using the tail-cuff method. Both the AngII and the AngII+Telmi groups showed no differences in heart rate among the genotypes (data not shown). Although *Rgs2*$^{-/-}$ mice tended to show a lower body weight than the other genotypes, drug administration did not affect the body weight (data not shown).

Survival rates and blood biochemical examinations

Some mice died during the period of administration mainly because of the cardiovascular events, including the rupture of aneurysms. Therefore, we compared the survival curves in mice with all Rgs2 genotypes and with the three treatment groups. As shown in Figure 2, AngII treatment decreased the survival rate for all the Rgs2 genotypes compared with the control group, but there were no significant differences in survival rate among the Rgs2 genotypes in the AngII group. Interestingly, *Rgs2*$^{-/-}$ mice treated with AngII+Telmi had significantly improved survival compared with *Rgs2*$^{-/-}$ mice treated with AngII alone (P<0.05).

As shown in the Table 1, blood urea nitrogen levels were significantly increased in the AngII and AngII+Telmi groups compared with the control group (P<0.05). Creatinine levels also tended to increase in the AngII group compared with the control group. These results indicated the exacerbation of renal function caused by AngII-induced hypertension in all Rgs2 genotypes. Recent studies have shown that telmisartan improves the metabolism of lipids and glucose.[22,23] Our study showed that low-density lipoprotein-cholesterol levels were significantly decreased in the AngII+Telmi group compared with the

Table 1 Biochemical examinations of serum samples

	Rgs2	*Control*	*AngII*	*AngII+Telmi*
BUN (mg dl^{-1})	+/+	27.2±2.9	57.1±4.6*	51.7±1.8*
	+/−	23.8±1.9	52.7±2.2*	48.8±3.7*
	−/−	29.4±4.3	47.8±2.3*	51.0±2.6*
CRE (mg dl^{-1})	+/+	0.07±0.00	0.12±0.01*	0.09±0.01*
	+/−	0.06±0.01	0.13±0.01*	0.10±0.01*
	−/−	0.06±0.01	0.10±0.01	0.08±0.01
LDL-C (mg dl^{-1})	+/+	2.0±0.0	3.1±0.3	4.9±0.7
	+/−	2.4±0.4	4.1±0.4	2.8±0.3
	−/−	5.0±1.2	6.0±1.4	3.1±0.5†
GLU (mg dl^{-1})	+/+	108.4±14.4	93.6±11.7	98.6±14.1
	+/−	112.4±23.8	103.5±10.4	109.5±10.7
	−/−	70.8±7.2	72.2±9.7	88.9±8.1

Abbreviations: AngII, angiotension II; BUN, blood urea nitrogen; CRE, creatinine, LDL-C, low-density lipoprotein-cholesterol; GLU, glucose, Rgs2, regulator of G-protein signaling 2; Telmi, telmisartan.
Results are expressed as mean ± s.e.m. in the control group (*Rgs2*$^{+/+}$: n=5, *Rgs2*$^{+/-}$: n=5, *Rgs2*$^{-/-}$: n=5), the AngII group (*Rgs2*$^{+/+}$: n=11, *Rgs2*$^{+/-}$: n=21, *Rgs2*$^{-/-}$: n=12) and the AngII+Telmi group (*Rgs2*$^{+/+}$: n=14, *Rgs2*$^{+/-}$: n=15, *Rgs2*$^{-/-}$: n=15). *P<0.05, *vs.* the control group. †P<0.05, *vs.* the AngII group.

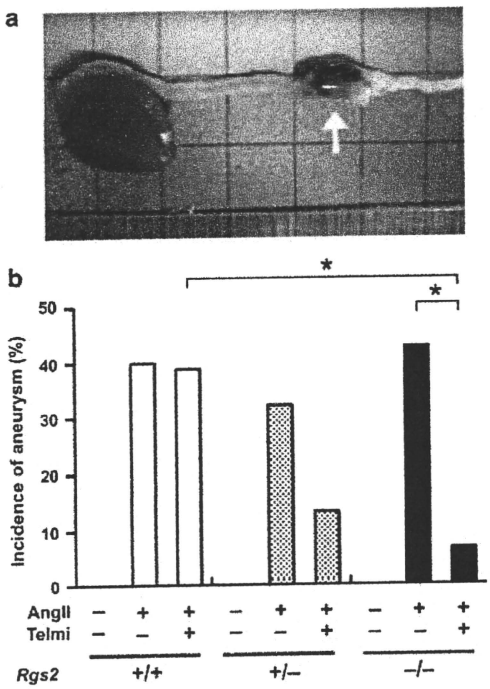

Figure 3 Gross morphology and incidence of aortic aneurysms observed in mice treated with AngII or AngII plus telmisartan. (**a**) Representative photograph showing the macroscopic features of aneurysm induced by AngII treatment. Aneurysm is indicated by arrow. (**b**) The incidence of aneurysms is expressed as a percent of animals in the control group ($Rgs2^{+/+}$: n=8, $Rgs2^{+/-}$: n=8, $Rgs2^{-/-}$: n=9), the AngII group ($Rgs2^{+/+}$: n=20, $Rgs2^{+/-}$: n=28, $Rgs2^{-/-}$: n=21) and the AngII+Telmi group ($Rgs2^{+/+}$: n=18, $Rgs2^{+/-}$: n=15, $Rgs2^{-/-}$: n=15). *P<0.05.

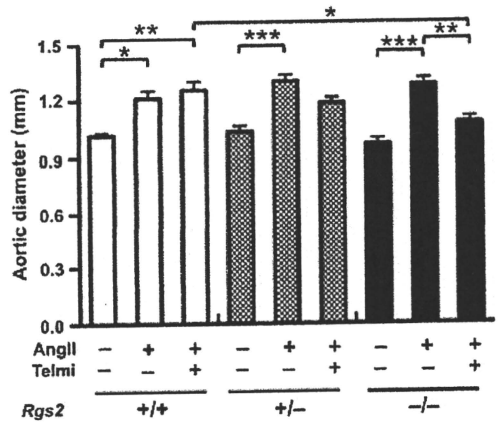

Figure 4 Comparison of abdominal aortic diameters in mice treated with AngII or AngII plus telmisartan. Diameter was measured in the middle of the abdominal aorta between the diaphragm and the renal artery bifurcation, and was compared. Results are expressed as mean ± s.e.m. in the Control group ($Rgs2^{+/+}$: n=8, $Rgs2^{+/-}$: n=8, $Rgs2^{-/-}$: n=8), the AngII group ($Rgs2^{+/+}$: n=12, $Rgs2^{+/-}$: n=19, $Rgs2^{-/-}$: n=11) and the AngII+Telmi group ($Rgs2^{+/+}$: n=10, $Rgs2^{+/-}$: n=13, $Rgs2^{-/-}$: n=14). *P<0.05, **P<0.01, ***P<0.001.

AngII group in $Rgs2^{-/-}$ mice (P<0.05), whereas no changes in glucose levels were observed. Liver function, as indicated by aspartate aminotransferase, alanine aminotransferase and lactate dehydrogenase levels, was normal (data not shown).

Vascular remodeling

In the AngII group, ~30–40% of mice had aortic aneurysms, as shown in Figure 3a. The incidence of aortic aneurysm was not different among Rgs2 genotypes in the AngII group. $Rgs2^{-/-}$ mice treated with AngII+Telmi had a significantly lower rate of aneurysm formation than the AngII group (P<0.05, Figure 3b). In $Rgs2^{+/-}$ mice, the AngII+Telmi group had a lower rate of aneurysm than the AngII group. Moreover, the incidence of aortic aneurysms in $Rgs2^{-/-}$ mice was significantly lower than that in $Rgs2^{+/+}$ mice in the AngII+Telmi group (P<0.05).

Next, we compared the diameters of the abdominal aorta (Figure 4). The AngII group showed significantly more enlarged aortic diameters than the control group for all Rgs2 genotypes ($Rgs2^{+/+}$: P<0.05, $Rgs2^{+/-}$, $Rgs2^{-/-}$: P<0.001). Although AngII+Telmi treatment did not reduce blood pressure in any of the genotypes, it significantly reduced enlargement of the aortic diameter compared with the AngII treatment of $Rgs2^{-/-}$ mice (P<0.01). In addition, in $Rgs2^{+/-}$ mice the AngII+Telmi treatment tended to reduce the enlargement of the aortic diameter compared with AngII treatment alone.

Oxidative stress in vascular walls

To assess oxidative stress in the aortic wall, we measured superoxide production and NAD(P)H oxidase activity. Figure 5A shows the *in situ* detection of superoxide in the abdominal aorta using dihydroethidium staining in $Rgs2^{-/-}$ mice. The red fluorescence intensity of the aorta in $Rgs2^{-/-}$ mice tended to be more intense in the AngII group and was obviously suppressed in the AngII+Telmi group. Quantitative analysis showed that superoxide production of the aorta in $Rgs2^{-/-}$ mice was significantly decreased in the AngII+Telmi group compared with the AngII group (P<0.001), whereas production in the other Rgs2 genotypes was not statistically different (Figure 5B). Furthermore, the NAD(P)H oxidase activity of aorta in $Rgs2^{-/-}$ mice was also decreased in the AngII+Telmi group compared with the AngII group (P<0.001, Figure 5c).

DISCUSSION

This study showed that the AngII group exhibited higher systolic blood pressure, a higher mortality rate, a higher aortic aneurysm incidence, and a more enlarged aortic diameter than the control group for all Rgs2 genotypes. Interestingly, in $Rgs2^{-/-}$ mice, the AngII+Telmi group showed a significant improvement in the survival rate as well as in the suppression of vascular remodeling compared with the AngII group, although blood pressure was not changed. In parallel with this improvement of vascular phenotypes in $Rgs2^{-/-}$ mice, the NAD(P)H oxidase activity and superoxide production of the aorta in $Rgs2^{-/-}$ mice was decreased in the AngII+Telmi group. Thus, low-dose telmisartan could prevent AngII-induced vascular remodeling via the suppression of oxidative stress in the vascular wall of $Rgs2^{-/-}$ mice.

Rgs2 dysfunction is expected to enhance the AngII signaling through AT_1R, leading to blood pressure elevation, atherosclerotic vascular remodeling and organ damage. However, our results did not show significant differences among Rgs2 genotypes in the AngII group, including blood pressure, mortality rate, aneurysmal formation, aortic diameter and aortic oxidative stress (Figures 1–5). The reason for the lack of differences among the Rgs2 genotypes may have been because the concentrations and dosing period of AngII may be excessive and outside the capability of Rgs2 regulation. Nevertheless, AngII was given in doses sufficient to cause the